

University of Nebraska - Lincoln

DigitalCommons@University of Nebraska - Lincoln

Department of Biological Systems Engineering: Dissertations and Theses Biological Systems Engineering, Department of


8-2020

Development of Novel Catalysts for Hydrogen Gas production from Biomass Compounds

Boanerges Bamaca

University of Nebraska-Lincoln, bbamaca@huskers.unl.edu

Follow this and additional works at: <https://digitalcommons.unl.edu/biosysengdiss>

 Part of the [Bioresource and Agricultural Engineering Commons](#), and the [Catalysis and Reaction Engineering Commons](#)

Bamaca, Boanerges, "Development of Novel Catalysts for Hydrogen Gas production from Biomass Compounds" (2020). *Department of Biological Systems Engineering: Dissertations and Theses*. 156. <https://digitalcommons.unl.edu/biosysengdiss/156>

This Thesis is brought to you for free and open access by the Biological Systems Engineering, Department of at DigitalCommons@University of Nebraska - Lincoln. It has been accepted for inclusion in Department of Biological Systems Engineering: Dissertations and Theses by an authorized administrator of DigitalCommons@University of Nebraska - Lincoln.

DEVELOPMENT OF NOVEL CATALYSTS FOR HYDROGEN GAS PRODUCTION
FROM BIOMASS COMPOUNDS

by

Boanerges Elias Bamaca Saquic

A THESIS

Presented to the Faculty of
The Graduate College at the University of Nebraska
In Partial Fulfillment of Requirements

For the Degree of Master of Science
Major: Agricultural and Biological Systems Engineering

Under the Supervision of Professor Sibel Irmak and Professor Mark Wilkins

Lincoln, Nebraska

August, 2020

DEVELOPMENT OF NOVEL CATALYSTS FOR HYDROGEN GAS PRODUCTION FROM BIOMASS COMPOUNDS

Boanerges Elias Bamaca Saquic, MS.

University of Nebraska, 2020

Advisors: Sibel Irmak and Mark Wilkins

Hydrothermal biomass gasification technologies (sub- and supercritical water gasification and aqueous-phase reforming) have considerable economic, environmental, and technical advantages over other energy-extensive technologies (e.g. natural gas reforming) for hydrogen gas production. However, lack of economically feasible and highly active catalysts is a main challenge that impedes upscaling of these technologies for hydrogen gas production.

The goal of this study was to develop innovative, economically feasible and active heterogeneous supported metal catalysts for hydrothermal processes for producing hydrogen gas from biomass-derived compounds. Because of its stable structure and chemical inertness, graphene was used as catalyst support. Graphene supported metal catalysts were prepared using different Pt precursors ($\text{H}_2\text{PtCl}_6 \cdot 6\text{H}_2\text{O}$, PtBr_2 , PtCl_2 , and PtI_2) and different metals in monometallic (Pt, Ni and W) and bimetallic (Pt-Ni and Pt-W) combinations for hydrothermal gasification of biomass compounds. The catalysts were prepared by wet impregnation and ultrasound-assisted wet impregnation for comparison. Sequential reduction methods (first chemical reduction with NaBH_4 then

thermal reduction with heating at 300 °C under nitrogen flow) were applied to reduce metal precursors on the support. Catalytic activity of the catalysts were tested by aqueous-phase reforming (APR) as a low temperature hydrothermal gasification technology. Glucose as simple biomass compound was used as feed in APR process.

It was found that the size and distribution of metal particles on the graphene support were highly dependent on the metal type and the metal precursor used in the preparation of the catalysts. The 8 wt.% of metal loading was successfully achieved in all catalysts when ultrasound-assisted wet impregnation deposition method was used. When catalyst was prepared using PtCl_2 precursor, the sizes and distributions of Pt particles on graphene were relatively small and uniform with narrow dispersion compared to the catalysts prepared with PtI_2 , PtBr_2 and H_2PtCl_2 precursors. Deposition of W particles on graphene exhibited better results than Ni catalysts in terms of metal particle size and distribution. APR results showed that use of different Pt precursor did not change catalytic activity of Pt/graphene catalysts in terms of total gas mixture and hydrogen produced in APR process if ultrasonication was used in wet impregnation process. Combination of Ni and W metals with Pt showed positive synergy and the catalytic performance of bimetallic catalysts was significantly enhanced.

ACKNOWLEDGMENTS

I would like to thank my advisor, Dr. Sibel Irmak for sharing her knowledge, patience, and professional experience; and thus, allowing me the freedom to be academically creative and productive during this process. Additionally, this would have not been possible without the help of my co-advisor, Dr. Mark Wilkins, whom I believe, truly enjoys what he does and is always willing to lend a helping hand and share from his professional experience. Besides my advisors, I would like to thank my other committee member, Dr. Martha Morton for her helpful advice and comments in my thesis. I would also like to thank Dr. Thomas Smith who is Assistant Director Research Instrumentation in Chemistry for helping me on running characterization analysis of my samples.

Being part of the University of Nebraska-Lincoln and being a Husker is something that I will cherish for the rest of my life. I am deeply thankful to UNL and to the Biological Systems Engineering Department and faculty for granting me this, once in a lifetime, opportunity to grow academically and professionally.

My family has been the strongest support someone could ask for. I am very thankful for my dad, Boanerges and my mother Maria, it is through their effort and encouragement that I have kept moving forward. I am also blessed to have wonderful siblings, Jocabed, Melanie and Jesua, I am thankful for them and their lovely families.

Many of my friends have been constantly looking after me, I am thankful for their lives, the ones back in Guatemala and the ones here. I would not have made it this far without them. All of them, either from college, Church, or any other place I have met them.

Lastly, and more importantly, I thank God for this. To Him be the glory.

Table of Contents

LIST OF TABLES	iv
LIST OF FIGURES	iv
CHAPTER 1. INTRODUCTION AND OBJECTIVES OF RESEARCH.....	1
1.1 Biofuels and hydrogen gas as a biofuel.....	1
1.2 Hydrogen gas production from biomass	2
1.2.1 Hydrothermal gasification process for hydrogen gas production.....	3
1.3 Catalyst.....	5
1.3.1 Types of catalytic reactions	7
1.3.1.1 Homogeneous.....	7
1.3.1.2 Heterogeneous catalysts	7
1.4 Importance of catalyst in production of biofuels and bioproducts.....	9
1.4.1 Importance of the catalyst for hydrogen gas production	9
1.4.2. Impregnation method for preparation of supported metal catalysts	11
1.4.3 Carbon materials as catalyst support	13
1.5 Objectives.....	17
1.6 Thesis Organization.....	18
References	20
CHAPTER 2. PREPARATION AND CHARACTERIZATION OF THE CATALYSTS	25
2.1 Introduction	26
2.2 Materials and Methods	28
2.2.2 Characterization of the catalysts.....	30
2.3 Results and Discussion.....	31
2.3.1 Characterization of graphene before and after being used as a catalyst support	31
2.3.2 Amounts of metals deposited on graphene.....	34
2.3.3 TEM images	36
2.3.4. XRD of the catalysts.....	39
2.3.5 Surface area and pore volume comparisons of the catalysts	41
2.4 Conclusion.....	43
References	44
CHAPTER 3. EVALUATION OF THE CATALYSTS FOR CONVERSION OF BIOMASS COMPOUNDS TO HYDROGEN GAS BY APR	47
3.1 Introduction	48
3.2 Materials and Methods	50
3.2.1 Catalysts.....	50
3.2.2 Evaluation of the catalysts by APR	51

3.2.3 Statistics analysis.....	52
3.3 Results and Discussion.....	53
3.3.1 Effect of Pt precursor types on the activity of Pt-graphene catalyst	53
3.3.2 Effect of different metals and their bimetallic combinations with Pt.....	56
3.4 Conclusion.....	58
References	59
CHAPTER 4: CONCLUSIONS AND SUGGESTIONS FOR FUTURE RESEARCH..	61
References	63

LIST OF TABLES

Table 2.1. Metal precursors used for the preparation of the catalysts.	29
Table 2.2. Comparison of theoretical and actual Pt amount deposited on the support* ...	34
Table 2.3. Comparison of theoretical and actual metal amounts deposited on the graphene by ultrasound-assisted wet impregnation method*	35
Table 2.4. Comparison surface areas and pore volumes of the catalysts prepared with different Pt precursors	42
Table 2.5. Comparison of surface areas and pore volumes of the catalysts prepared with different metals	43
Table 3.1. APR results of the catalysts prepared with different Pt precursors (non-sonicated)*	54
Table 3.2. APR results of the catalysts prepared with different Pt precursors by ultrasound-assisted impregnation technique*	54
Table 3.3. APR results of the catalysts prepared with different metals and combination of these metals with Pt*	57

LIST OF FIGURES

Figure 1.1. Conventional hydrogen production from biomass pathways (Milne, Elam, & Evans).	3
Figure 1.2. The effect of catalyst on a reaction (exothermic reaction)	6
Figure 1.3. Field emission microscope images of three types of catalyst supports demonstrating different morphologies and dimensions: (a) graphene, (b) graphite, and (c) carbon black. Images are presented at magnifications appropriate for demonstration of support features (Dong, Gari, Li, Craig, & Hou, 2010).....	14
Figure 1.4. Chemical structure of graphene (Perreault, Fonseca De Faria, & Elimelech, 2015).	15
Figure 1.5. Graphical description of graphene sheet fluctuations (Meyer, et al., 2007)... ..	16
Figure 2.1. Infrared spectra of graphene samples (No baseline correction was applied). ..	32
Figure 2.2. Structures of graphene and graphene oxide (Perreault, Fonseca de Faria, & Elimelech, 2015).	32
Figure 2.3. Raman spectra of graphene samples.....	33
Figure 2.4. TEM images, EDS spectra and particle size distributions of non-sonicated (a) and sonicated (b) catalysts prepared using PtI ₂ precursor.	37
Figure 2.5. TEM images and particle size distributions of the catalysts prepared with different platinum precursors by application of sonication.	38
Figure 2.6. TEM images and particle size distributions of the catalysts prepared with different metals.	38
Figure 2.7. XRD patterns of the catalysts prepared with different Pt precursors.	39
Figure 2.8. XRD patterns of the catalysts prepared with different metals.....	40

Figure 3.1. Hydrogen percentages of the gas mixtures produced and hydrogen yield obtained in mono and bimetallic catalysts.	58
---	----

CHAPTER 1. INTRODUCTION AND OBJECTIVES OF RESEARCH

1.1 Biofuels and hydrogen gas as a biofuel

The depletion of fossil fuel resources and the effects and concern of climate and change has forced the countries to transition to renewable and cleaner energy technologies such as wind and solar energy. However, for moving vehicles, it remains necessary to have liquid or gas fuels, such as bioethanol, biodiesel and hydrogen. Bioethanol is a liquid biofuel produced through fermentation of glucose and other sugars in the corn, sugarcane or other crops and biomass. The use of ethanol as a fuel source goes back to the first ideas to power an engine. Henry Ford had the idea to power his Ford model T on pure ethanol, which nowadays remains as a very profitable industry and it is even a requirement by the U.S government, through the Renewable Fuel Standard (RFS) (US Department of energy, n.d.), to contain a minimum ethanol content in renewable fuels.

Biodiesel is a renewable, biodegradable liquid fuel produced from vegetable oils and animal fats. Because of having higher flashpoint than petroleum diesel it is safer fuel to store and transport. It can be used in diesel engines with almost no modifications. Two main of the drawbacks of this biofuel are (i) it begins to solidify in cold conditions and (ii) quality of the biodiesel is highly dependent on the main characteristics of the raw materials such as contents and compositions of oils/fats used in the manufacture of biodiesel.

Hydrogen gas is a renewable gas biofuel that is converted to electricity by fuel cells. Hydrogen has zero greenhouse gases emissions. It generates large amounts of energy per unit weight during combustion. In other words, it has the highest specific

energy content of all conventional fuels (Wiltowski, Mondal, Campen, Dasgupta, & Konieczny, 2008). Its only waste or byproduct is pure water. Most hydrogen produced in the United States is made by natural gas reforming, which is an energy extensive process taking place at very high temperatures (700°C-1,000°C). The full environmental and economic benefits of generating power from hydrogen are achieved when hydrogen is produced from renewable sources rather than natural gas and coal with an effective and suitable method. Developing new catalysts with novel properties is one of the greatest concerns and potential impediments for hydrogen production from sustainable and abundant feedstock, biomass.

1.2 Hydrogen gas production from biomass

There is growing interest in obtaining hydrogen from several different low-cost substrates such as biomass, wastewaters, algae, agricultural feedstocks and agricultural wastes (Wang & Yin, 2018). There is a lack of efficient hydrogen production from biomass methods and technologies, even though biomass is the one of the largest feedstocks for hydrogen gas production. There are three basic categories for the production of hydrogen from biomass: biological, thermochemical and photolytic processes. Figure 1 summarizes two of the main conventional types of hydrogen production techniques, not including photolytic processes. In many cases, due to large water content and high drying cost, biomass is not a suitable feedstock for conventional thermochemical gasification technologies. Thermochemical gasification techniques such as biomass gasification and pyrolysis are energy-intensive processes and produce relatively high amounts of char and tar with low conversion of biomass into gas. On the other hand, hydrothermal gasification, using super- or subcritical water as the reaction

medium, is seen as a very promising and viable way of producing hydrogen from biomass with high efficiency.

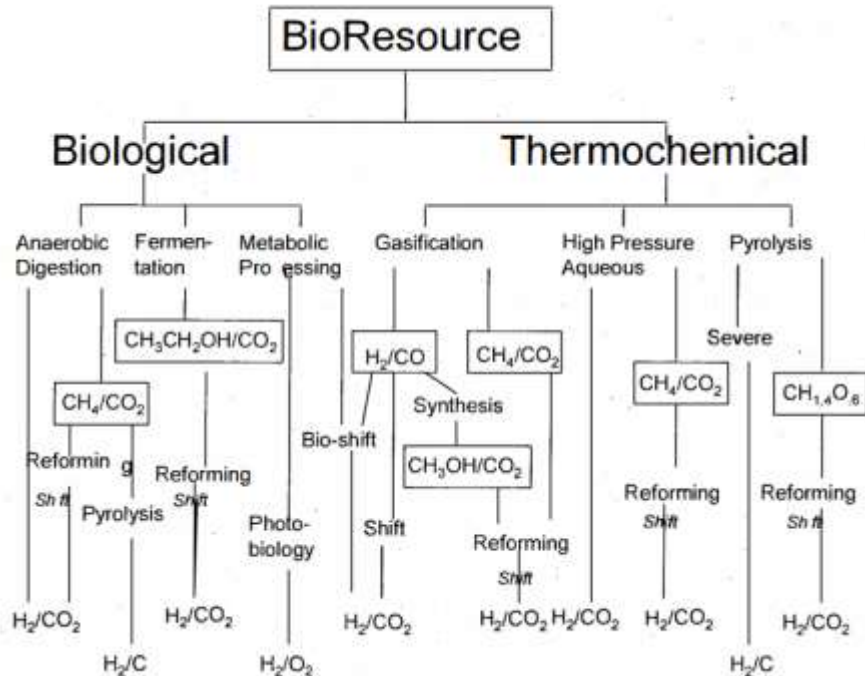


Figure 1.1. Conventional hydrogen production from biomass pathways (Milne, Elam, & Evans).

1.2.1 Hydrothermal gasification process for hydrogen gas production

In hydrothermal gasification process, the gasification reactions take place in hot compressed water. Based on reaction temperatures and pressure, water can be in supercritical state or subcritical liquid in the process. Use of non-edible lignocellulosic biomass in hydrothermal conversion processes is attracting increasing attention as renewable, economical, and abundant resources to reduce minimize energy and material feedstock costs. In general, due to complete gasification in a short reaction, hydrothermal gasification technologies are considered cost-effective and efficient gasification

technologies for wet feedstock, such as biomass. Depending on the temperature range, hydrothermal biomass gasification processes are divided into three main types:

- ✓ supercritical water biomass gasification
- ✓ subcritical water biomass gasification
- ✓ low temperature biomass gasification (aqueous-phase reforming, APR).

The chemical properties of water are greatly changed at high temperatures and pressures due to the reduction of hydrogen bonding, which causes changes in dissociation, solubility, diffusivity, and reactivity (Kruse & Dinjus, 2007). Subcritical water has a lower relative dielectric constant and a higher ionic product than ambient water. When the temperature of water increases from ambient temperature to 250 °C, its relative dielectric constant decreases from around 80 to nearly 27 (Herrero, Cifuentes, & Ibañez, 2006). Furthermore, the ion product of subcritical water substantially increases with temperature; therefore, subcritical water can catalyze chemical reactions such as hydrolysis, degradation and gasification (Rogalinski, Herrmann, & Brunner, 2005; Khajavi, Ota, Kimura, & Adachi, 2006).

When pressure is around 35 MPa and temperature is in sub- and supercritical regions under 400 °C, ionic product numbers of water (K_w) values are always higher than 1×10^{-14} . The K_w reaches its maximum value ($\sim 10^{-11}$) between 200-300 °C. The K_w does not respond to changes in pressure when in this temperature range. The molar concentrations of hydrogen ion (H^+) and hydroxide ion (OH^-) in these regions are almost 30 times higher than those under room temperature. Therefore, the hydrolysis, degradation and/or gasification yield in these regions is expected to be high (Glasser, 2004).

As a hydrothermal gasification technique, aqueous-phase reforming (APR) takes place in an aqueous medium at mild conditions (225-265 °C and 2.7-5.4 MPa), which reduces the cost of the procedure (Cortright, Davda, & Dumesic, 2002; Irmak & Öztürk, 2010). The cost of the process can be further reduced by using cheap but highly active catalysts.

Catalyst is a key parameter for production of hydrogen in higher yield and richer composition that could potentially reduce the cost of hydrogen production. In this matter, development of catalysts with novel properties is a challenge for economically feasible hydrogen gas production by hydrothermal biomass gasification processes.

1.3 Catalyst

Catalyst is a substance that increases the rate of a reaction, when compared to the same reaction without this substance. A catalyst increases the reaction rate without getting consumed in the process. From a thermodynamics point of view, this is achieved by reducing the overall activation energy change that occurs during the reaction. This process is known as catalysis. For a catalysis, the catalyst is a reactant and also a product since there is no chemical change on its structure (Laidler, 1996). A physicochemical understanding of how a catalyst works is very useful to determine the steps of how catalysis reaction takes place over time and the importance of the concept of activation energy (E_{act}). E_{act} is a minimum energy that is needed for a reaction to take place. Generally, the rate of the reaction is inversely proportional to the E_{act} . The higher reaction rate is expected throughout the overall reaction when the E_{act} is lower. The final energy difference of the overall reaction can be measured as a change of enthalpy, known also as the heat of reaction (ΔH). A catalyst reduces the E_{act} or changes the reaction mechanism involving a different transition state of lower energy. An important concept,

but somehow counterintuitive, is that the catalyst does not affect the enthalpy and free energy in both, the initial and final states. The catalyst will increase and facilitate the interaction among the participating particles in the reaction. Therefore, a catalyst cannot make a thermodynamically unfavorable reaction happen, and ΔH , ΔG and the equilibrium constant (k) will not change due to the catalyst (Bartholomew & Farrauto, 2005).

A catalyst reduces the activation energy for a given reaction in two ways:

- orienting the reactant compounds for successful collisions to facilitate the reaction.
- reacting with the reactants to lead to formation of an intermediate (called activated complex) that requires lower energy to produce the product(s)

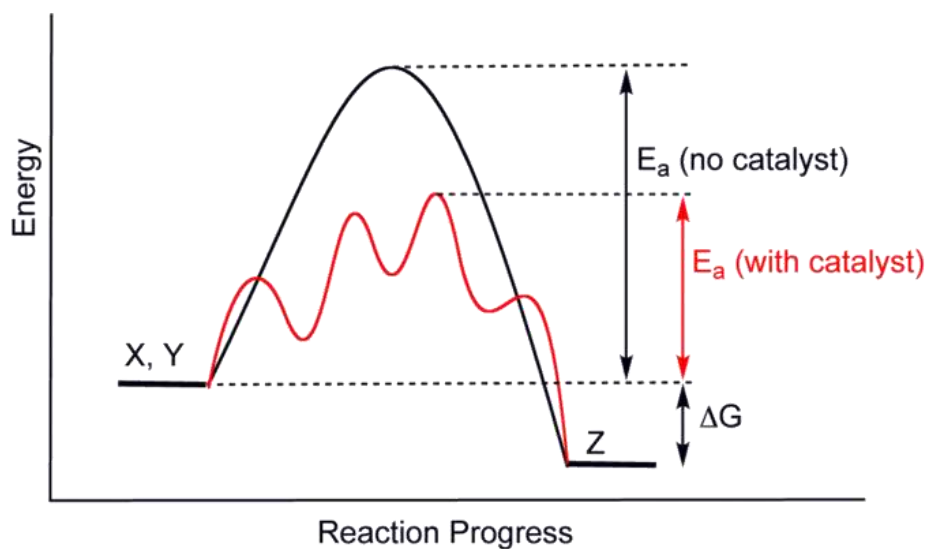


Figure 1.2. The effect of catalyst on a reaction (exothermic reaction)

(Retrieved June 5, 2020 from:
<https://courses.lumenlearning.com/boundless-chemistry/chapter/catalysis/>)

1.3.1 Types of catalytic reactions

Catalysts can be divided into two groups depending on phase and catalysts in the reaction mixture: homogeneous and heterogeneous catalysts.

1.3.1.1 Homogeneous catalyst

In a homogeneous catalyst system, the catalyst and reactants are in the same phases which can be single liquid phase or gas phase. Homogeneous catalysts can be Brønsted and Lewis acids, metals ions, organometallic complexes, acid-bases and enzymes which catalyze biological reactions. Recovery of homogeneous catalysts usually is difficult and generally requires an expensive process. In general, homogeneous catalysts have poor thermal stability. However, their single active site shows excellent selectivity for a specific reaction. When comparing heterogeneous catalyst to homogeneous catalyst, the latter tend to have higher activity and selectivity. These also work well under mild reaction conditions and have lower sensibility to catalyst poison.

1.3.1.2 Heterogeneous catalysts

The complete catalytic system encompasses the reagents, catalyst and products. The reaction occurs at the interphase between phases (Laidler, 1996), from this it is possible to understand that the heterogeneous catalyst is not in the same phase of the reactants and the substance. Heterogeneous catalysts are mostly solids that are added into gas or liquid reaction mixtures. Only certain sites on the catalyst surface participate in the reaction that are called active sites. The reactant compounds are adsorbed onto these active sites on the surface of the catalyst for facilitating any reaction. Activity of the catalyst is dependent on the number of these active sites available on the catalyst's

surface and is expressed with turnover frequency. Turnover frequency: number of molecules reacting per active site per second at a certain reaction condition.

Heterogeneous catalyst is adequate to be used in a multistage reaction process; this would not be possible with a homogenous one. The exact mechanism of the heterogeneous catalysis pathway still needs further research for individual cases since it may have several variables that add complexity, such as catalyst metal, support and reaction conditions, however, the general elementary steps can be described by Sabatier's catalyst law (van Santen, 2010).

- The catalyst surface adsorbs the reactant molecules. These molecules become activated and produce intermediate reaction complexes.
- Through different processes, depending on the catalyst material, the complexes produced rearrange and recombine into new molecules.
- Desorption of the product molecules occurs on the catalyst surface, which frees the catalyst surface again.

For a reaction $A + B \rightleftharpoons C$, from Sabatier's law describes that the nature of a heterogeneous catalytic system is cyclic. The difficulty in determining a general detailed mechanistic explanation lays in the fact that the reaction activation rates for A and B, the type and rate of formation of AB intermediate product molecules, and the consequent desorption of C from the catalyst surface all compete during the time the reaction occurs.

The main advantages of heterogeneous catalysts are (i) recovery is easy and cheap (e.g. separation with filtration and centrifugation), (ii) thermal stability is good, and (iii) they can have multiple active sites.

1.4 Importance of catalyst in production of biofuels and bioproducts

The selection and use of catalysis are paramount to the continuity of any type of industry or biological process for production of value-added products including biofuels and bioproducts. For example, at the end of pyrolysis, the use of catalyst is known as catalytic pyrolysis and it allows the thermal decomposition of biomass to obtain a higher quantity and quality of products. The first generation biofuels obtained from biomass usually contain a high percentage of oxygen, but the use of catalysts allows for de-oxygenation, de-carboxylation and dehydration of different types of biomass (Hornung, 2014).

During the production of bioethanol, which currently has become one of the most important biofuels, lignocellulosic biomass is hydrolyzed into sugar, which then is fermented to ethanol. There are other paths to achieve ethanol or other types of alcohol production. An important one is through a thermochemical process, where the biomass can also be gasified to produce syngas, which then, is converted into ethanol or other alcohols via catalytic reaction (Hornung, 2014).

1.4.1 Importance of the catalyst for hydrogen gas production

Different catalysts have produced different yields and using multifunctional catalysts and different reactions pathways can be useful to produce a wide range of products from carbohydrate based feedstock (Chheda, Huber, & Dumesic, 2007). A considerable amount of research has been carried with the aqueous-phase reforming (APR) technique (Valenzuela, Jones, & Agrawal, 2006).

It is possible to use organic materials and polymers in a heterogeneous catalyst as a support material, nonetheless, inorganic and simple carbon based materials are readily available and have been used as a catalytic support to produce hydrogen. These materials are considered to have an advantage due to the fact that they have following properties (Balcar & Roth, 2013)

- i. Higher thermal stability,
- ii. The pore characteristics of the materials is preserved, mostly resisting any swelling due to the use of solvents,
- iii. Porosity in the material is relatively constant,
- iv. Surface area of in the support material is high.

As previously mentioned, one of the variables to analyze for the design of a catalyst is the size of its support particles. There are a variety of materials that can be used as a catalyst support, but carbon products are among the most promising ones (Furimsky & Spivey, 2008). It was reported that smaller sized and narrower size distribution for the activated carbon support particles exhibited a higher activity and hydrogen selectivity (Meryemoglu, Irmak, Hasanoglu, Erbatur, & Kaya, 2014).

Platinum is considered one of the best catalysts for various aqueous-phase reactions (Rahman, Church, Variava, Harris, & Minett, 2014). Platinum is also a common metal catalyst for hydrogen gas production. Recent research activities show the efficiency of working with combinations of either two or three metals with platinum, such as ruthenium and tin. Working with different metals has the potential of lowering the production cost of hydrogen, since the price of platinum can be prohibitive for scaling up a process. Every new variable influences the hydrogen production, but while working

with different metallic catalysts, the other important variable is the type of support. Working with nanotubes presents a new window of research with results that show a relatively good catalytic activity for this type of setting (Kaya, Irmak, Hasanoğlu, & Erbatur, 2015).

1.4.2. Impregnation method for preparation of supported metal catalysts

The catalytic activity of a catalyst is strongly affected by the preparation method. The preparation of supported catalysts targets to attach the active phase onto the support. Impregnation is a well-known method in the development of heterogeneous catalysts such as supported metal catalysts. The precursor containing solution is contacted with the solid support and after adsorption of the precursor on the support the mixture is dried to remove the solvent. The solvent can be water or organic solvent or solvent mixtures depending on the solubility of the precursor. The precursor should include the metal(s) that is targeted to be deposited on the support. The precursors can be inorganic metal salts (e.g. metal sulfates, carbonates, halogens, nitrates, acetates) and organic metal complexes, such as metal acetylacetonates (Munnik, De Jongh, & De Jong, 2015).

There are two commonly used impregnation methods: wet impregnation and incipient wetness impregnation. In wet impregnation an excess of solution is used. After adsorption of precursor on the support, the excess solvent is removed by drying. In incipient wetness impregnation, the volume of the solution is equal or slightly less than the pore volume of the support. The amount of liquid is controlled by the solubility of the metal precursor. After the catalyst is impregnated onto the support, it is then dried. After drying process in impregnation methods, the adsorbed metal precursors are reduced and converted into the active phases by calcination.

Impregnation methods are fast and inexpensive; however, it is hard to achieve high dispersion of catalyst components on the support. It is also a challenge loading metals in fine size particles. To overcome these drawbacks many efforts have been applied and ultrasonic irradiation is a very effective one for heterogeneous catalysts (Burakova, Galunin, Rukhov, Memetov, & Tkachev, 2016).

The ultrasound effects of sonication in liquids, are understood by the cavitation effects of the rapid formation, growth and collapse of bubbles in the medium. There is a constant interaction between a solid phase (the heterogeneous catalyst), a liquid phase (the solution) and a gas phase (the gas bubbles), this interaction happens through energy exchanges, that are observed in gradients of temperature and pressure in very localized spots within each phase and within the inter-phase boundaries (Kuna, Behling, Valange, Chatel, & Colmenares, 2017). The main interaction happens through the formation and destruction of bubbles. However, these bubbles have no direct influence at the molecular level. The ultrasound frequency range is determined roughly between 15 kHz to 1 GHz, the wavelength then is around 10 to 10^{-4} cm, which is above the molecular size (Suslick, McNamara, & Didenko, 2001). This means that the high energy ultrasound effects of the sonicator are directly mechanical, the change on the general solution is mostly explained through mass transfer phenomena. There is, however, the possibility of chemical interaction, especially in the forms of chemisorption and ionic reactions, especially for heterogeneous systems (Colmenares, 2014; Cella, 2011).

When describing a heterogeneous reaction system, for ultrasound sonication, this refers to the liquid-solid-gas system during ultrasound energy interaction with a medium, in this case water with a supported catalyst, and not the type of catalytic system; although

some descriptive similarities are shared. In this type of system, the fundamental driver of change is diffusion and adsorption; this mass transfer phenomena increases the probability of ionic reactions to happen in the interphase of the liquid and the solid surface (Ince & Ziyilan, 2015). An improvement in the system is expected, primarily due to the erosion and deformation on the solid surface as a result of the violent turbulent mixing, cavitation, and the acoustic streams produced by asymmetric pressure differentials (Suslick, McNamara, & Didenko, 2001). By using sonication in the preparation of a heterogeneous catalyst, the dispersion of the metal nanoparticles is expected to be better across the carbon support; also, as a result of the interaction with the cavitation bubbles on the “hot spots” on the support, a higher deposition efficiency (DE) would generally be expected and a faster preparation with a lower energy input (Padilla, Priece, Lin, Lopez-Sanchez, & Zhong, 2017).

1.4.3 Carbon materials as catalyst support

Carbon-based materials include activated carbon, carbon nanotubes, mesoporous carbon, fullerenes, and graphene. Frequently, carbon materials have shown promising properties as catalyst supports for many reactions because of their good mechanical strength, thermal stability, high chemical stability, a large surface area, tailorable porous structure and surface chemistry. Carbon materials have been recognized as the most active supports for APR of biomass-derived compounds for hydrogen-rich gas production compared, among others, to alumina, titanium dioxide and silica. (Meryemoglu, Hesenov, Irmak, Atanur, & Erbatur, 2010).

Porous carbon materials are of interest in many applications due to their high surface area and physicochemical properties. These materials can be classified according to their pore

diameters as microporous (pore size < 2 nm), mesoporous (2 nm < pore size < 50 nm), and/or macroporous (pore size > 50 nm) (Liang, Li, & Dai, 2008). Mesoporous carbon materials have large surface areas and highly oxygen-functionalized surfaces. Those materials may offer great advantages over other carbon materials owing to their well-controlled pore structures in the mesopores. A group of carbon-based materials have the advantage of having several different allotropes, some of which have been used for centuries, such as graphite and diamonds. Recently, there has been new research in different fields of graphene (Julkapli & Bagheri, 2015) and nanotubes, which can also be considered a type of folded graphene. Nanotubes can be multi-walled or single walled, and this also may have an effect on the support selection for future catalysts (Dong, Gari, Li, Craig, & Hou, 2010).

Here is an example of three different types of carbon morphology for a catalyst support:

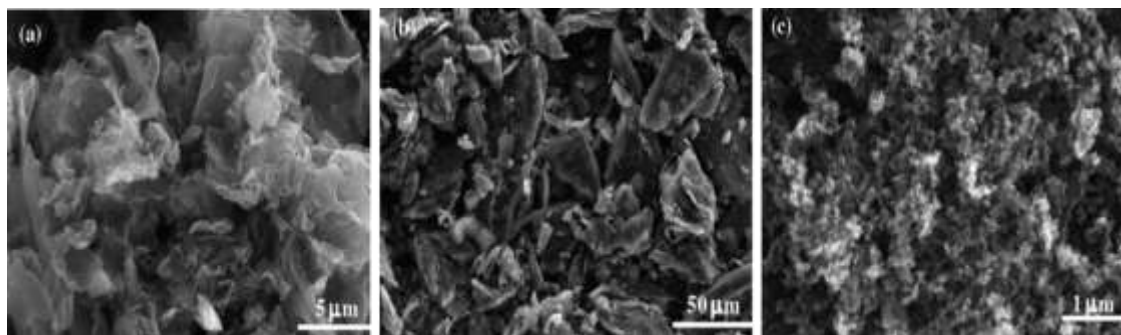


Figure 1.3. Field emission microscope images of three types of catalyst supports demonstrating different morphologies and dimensions: (a) graphene, (b) graphite, and (c) carbon black. Images are presented at magnifications appropriate for demonstration of support features (Dong, Gari, Li, Craig, & Hou, 2010).

1.4.3.1 Graphene as catalyst support

The chemical structure of graphene could be considered a basic structural element for different carbon allotropes (Hirsch, 2010), these include graphite, fullerenes, graphyne and carbon nanotubes. Amorphous types of carbons can also be considered to have graphene as a basic structure. Graphene is a two-dimensional carbon allotrope. It is composed of sp^2 -bonded carbon atoms arranged in a hexagonal structure (Figure 1.4.). Each carbon atom is covalently bonded to three other carbon atoms. Graphene is used in many fields as a promising building block material. Graphene has unique physicochemical properties such as great stability, high surface area, electron mobility, thermal conductivity, and mechanical strength. Graphene is the strongest known material.

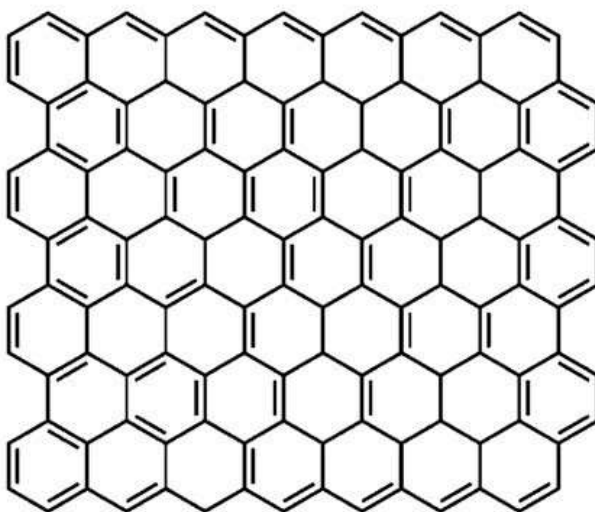


Figure 1.4. Chemical structure of graphene (Perreault, Fonseca De Faria, & Elimelech, 2015).

The 2D structure of graphene does not fold into different 3D structures after certain size and conditions. However, the structure is not completely flat, there is usually a large amount of fluctuation (Figure 1.5), of about 1 nm amplitude due to the carbon

bonds adaptation to thermodynamic fluctuations (Meyer, et al., 2007). After considering and visualizing graphene expected fluctuations, it is still useful to describe it as a 2D hexagonal lattice, that is one 0.35 nm, or one atom, thick, in which each atom is a vertex with sp^2 hybridization. The length of the carbon-carbon bond has been estimated to be 0.142 nm, the hexagonal stability of each ring is due to its three s bonds in each lattice. There is a p bond located vertically to the lattice plain, and it is responsible for the important electrical conductivity attributed to this material (Zhen & Zhu, 2017). The conductivity of graphene is considered one of the highest at room temperature, it has a conductivity of 10^6 S/m and a sheet resistance of 31 W/sq (Kim, et al., 2009).

Thermal conductivity is usually related to electrical conductivity, this is also the case for graphene, which at room temperature has a conductivity of about 5×10^3 W/m K, this is considerably higher than the thermal conductivity of copper (401 W/m K) (Balandin, et al., 2008).

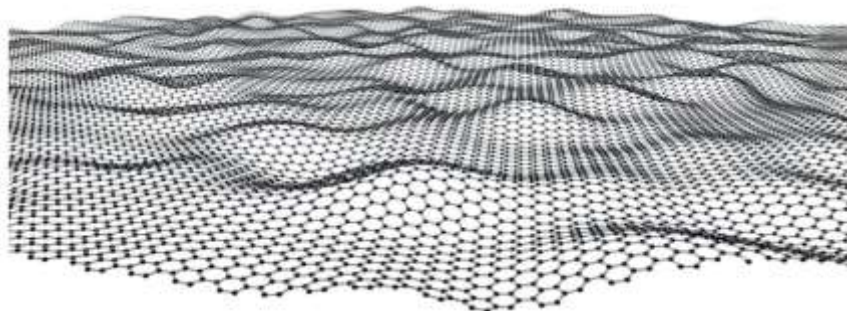


Figure 1.5. Graphical description of graphene sheet fluctuations (Meyer, et al., 2007)

When using graphene as a catalyst support, two important features to consider are, the surface area, that has been reported to reach $2630 \text{ m}^2/\text{g}$, (Stoller, Park, Yanwu, An, &

Ruoff, 2008) and its mechanical strength. The molecular stability of graphene is observed at a macro scale. Its crystal structures have shown a tensile strength of 125 GPa and an elastic modulus of 1.1 TPa (Lee, Wei, Kysar, & Hone, 2008). The reported strength limit can reach 42 N/m and, when comparing similar thickness, graphene has about 100 times the strength of steel (Stankovich, et al., 2006). Graphene provides different isolated layers, in between these layers molecules and nanoparticles could be deposited, adding a three-dimensional matrix to the support (Zhou, Chen, Wang, Sheng, & Xia, 2010). However, the p-p bonds between graphene sheets could cause the adherence of the isolated sheets and considerably reduce the number of particles that interact with its surface (Liu, et al., 2014). Research on this area suggest using polymers, carbon black, fullerenes, or other molecules with low surface area as spacers between graphene sheets (Tsoncheva, et al., 2013), this however, would require new preparation methods and further research.

1.5 Objectives

A very important part of the current research is focusing on the variables associated with the catalyst itself, such as the type of metal, the size of the metal catalyst particles on the support and effect of graphene as supportive material. The overall goal of this research is to develop new catalysts with novel properties to be used for sustainable hydrogen gas production from hydrothermal gasification of biomass.

The primary objectives are:

- I. To develop platinum-based supported metal catalysts (Pt and combinations of Pt with Ni and W) using graphene as a supportive material under sonicated and non-sonicated wet impregnation conditions.
- II. To determine properties of the catalysts with various techniques.
- III. To evaluate hydrogen gas production activity of the catalysts by aqueous-phase reforming of a biomass-derived compound, glucose.

1.6 Thesis Organization

Chapter I gives a brief introduction about biofuels, hydrogen gas as biofuel, hydrothermal gasification technologies, catalysts and carbon-based catalyst supports for hydrogen gas production.

Chapter II focuses on the characterization of the catalysts synthesized in the study using transmission electron microscopy (TEM), X-ray diffraction (XRD), Brunauer-Emmett-Teller (BET) surface area measurement, infrared (IR), Raman spectroscopy and inductively coupled plasma mass spectrometer (ICP-MS) techniques. Materials and methods were explained in detail, and the results (percent metal deposited, distribution of the metal particles on the support, particle size of the metal particles deposited, surface area, etc.) were presented and discussed.

Chapter III contains experimental procedures and results for activity of the catalysts for hydrogen gas production by APR. The catalysts were evaluated based on the total gas produced and hydrogen selectivity in the gas mixture that produced by gasification of aqueous glucose solution.

Chapter IV concludes overall results of the thesis and gives suggestions for future research.

References

- Balandin, A., Ghosh, S., Bao, W., Calizo, I., Teweldebrhan, D., Miao, F., & Lau, C. (2008). Superior thermal conductivity of single-layer graphene. *Nano Letters*, 8(3), 902-907.
- Balcar, H., & Roth, W. (2013). Hybrid catalysts for olefin metathesis and related polymerizations. En H. Balcar, & W. Roth, *New and Future Developments in Catalysis: Hybrid Materials, Composites, and Organocatalysts*, 1-26. Elsevier B.V.
- Bartholomew, C., & Farrauto, R. (2005). *Fundamentals of Industrial Catalytic Processes*. Hoboken, NJ, USA: John Wiley & Sons, Inc.
- Burakova, E.A., Burakov, A.E., Filatova, E.Y. et al. (2014). Effect of ultrasound on catalytic system for synthesizing carbon nanomaterials. *Theor Found Chem Eng* 48, 493–496.
- Cella, R. (2011). Ultrasound in synthetic applications and organic chemistry. En R. Cella, *Handbook on Applications of Ultrasound: Sonochemistry for Sustainability*, 263-279. CRC Press.
- Chheda, J., Huber, G., & Dumesic, J. (2007). Liquid-phase catalytic processing of biomass-derived oxygenated hydrocarbons to fuels and chemicals. *Angewandte Chemie - International Edition*.
- Colmenares, J. (2014). Sonication-induced pathways in the synthesis of light-active catalysts for photocatalytic oxidation of organic contaminants. *ChemSusChem*, 7(6), 1512-1527. Wiley-VCH Verlag.
- Cortright, R., Davda, R., & Dumesic, J. (2002). Hydrogen from catalytic reforming of biomass-derived hydrocarbons in liquid water. *Nature*, 418(6901), 964-967.
- Dong, L., Gari, R., Li, Z., Craig, M., & Hou, S. (2010). Graphene-supported platinum and platinum-ruthenium nanoparticles with high electrocatalytic activity for methanol and ethanol oxidation. *Carbon*.

- Furimsky, E., & Spivey, J. (2008). *Carbons and Carbon Supported Catalysts in Hydroprocessing*. The Royal Society of Chemistry.
- Glasser, L. (2004). Water, water, everywhere: Phase diagrams of ordinary water substance (J. Chem. Educ. (2004) 81, (414-418)). *Journal of Chemical Education*, 81(5), 414-418.
- Herrero, M., Cifuentes, A., & Ibañez, E. (2006). Sub- and supercritical fluid extraction of functional ingredients from different natural sources: Plants, food-by-products, algae and microalgae - A review. *Food Chemistry*, 98(1), 136-148.
- Hirsch, A. (2010). The era of carbon allotropes. *Nature Materials*, 9(11), 868-871. Nature Publishing Group.
- Hornung, A. (2014). *Transformation of Biomass*. (A. Hornung, Ed.) Chichester, UK: John Wiley & Sons, Ltd.
- Ince, N., & Ziyilan, A. (2015). Single and Hybrid Applications of Ultrasound for Decolorization and Degradation of Textile Dye Residuals in Water. En N. Ince, & A. Ziyilan, *Green Chemistry for Dyes Removal from Wastewater*, 261-293. Hoboken, NJ, USA: John Wiley & Sons, Inc.
- Irmak, S., & Öztürk, L. (2010). Hydrogen rich gas production by thermocatalytic decomposition of kenaf biomass. *International Journal of Hydrogen Energy*, 35(26), 5312-5317.
- Julkapli, N., & Bagheri, S. (2015). Graphene supported heterogeneous catalysts: An overview. *International Journal of Hydrogen Energy*, 40(2), 948-979.
- Kaya, B., Irmak, S., Hasanoğlu, A., & Erbatur, O. (2015). Developing Pt based bimetallic and trimetallic carbon supported catalysts for aqueous-phase reforming of biomass-derived compounds. *International Journal of Hydrogen Energy*.
- Khajavi, S., Ota, S., Kimura, Y., & Adachi, S. (2006). Kinetics of maltooligosaccharide hydrolysis in subcritical water. *Journal of Agricultural and Food Chemistry*(54), 3663-3667.

- Kim, K., Zhao, Y., Jang, H., Lee, S., Kim, J., Kim, K., . . . Hong, B. (2009). Large-scale pattern growth of graphene films for stretchable transparent electrodes. *Nature*, 457(7230), 706-710.
- Kruse, A., & Dinjus, A. (2007). Hot compressed water as reaction medium and reactant: Properties and synthesis reactions. *Journal of supercritical fluids*(39), 362-380.
- Kuna, E., Behling, R., Valange, S., Chatel, G., & Colmenares, J. (2017). Sonocatalysis: A Potential Sustainable Pathway for the Valorization of Lignocellulosic Biomass and Derivatives. *Topics in Current Chemistry*, 375(2). Springer Verlag.
- Laidler, K. (1996). A glossary of terms used in chemical kinetics, including reaction dynamics (IUPAC Recommendations 1996) in: Pure and Applied Chemistry Volume 68 Issue 1 (1996). *International Union of Pure and Applied Chemistry*, 68(1), 149-192.
- Lee, C., Wei, X., Kysar, J., & Hone, J. (2008). Measurement of the elastic properties and intrinsic strength of monolayer graphene. *Science*, 321(5887), 385-388.
- Liang, C., Li, Z., & Dai, S. (2008). Mesoporous carbon materials: Synthesis and modification. *Angewandte Chemie - International Edition*, 47(20), 3696-3717. John Wiley & Sons, Ltd.
- Liu, M., Song, Y., He, S., Tjiu, W., Pan, J., Xia, Y., & Liu, T. (2014). Nitrogen-doped graphene nanoribbons as efficient metal-free electrocatalysts for oxygen reduction. *ACS Applied Materials and Interfaces*, 6(6), 4214-4222.
- Meryemoglu, B., Hesenov, A., Irmak, S., Atanur, O., & Erbatur, O. (2010). Aqueous-phase reforming of biomass using various types of supported precious metal and raney-nickel catalysts for hydrogen production. *International Journal of Hydrogen Energy*.
- Meryemoglu, B., Irmak, S., Hasanoglu, A., Erbatur, O., & Kaya, B. (2014). Influence of particle size of support on reforming activity and selectivity of activated carbon supported platinum catalyst in APR. *Fuel*.
- Meyer, J., Geim, A., Katsnelson, M., Novoselov, K., Booth, T., & Roth, S. (2007). The structure of suspended graphene sheets. *Nature*, 446(7131), 60-63.

- Milne, T., Elam, C., & Evans, R. (s.f.). *Hydrogen from Biomass State of the Art and Research Challenges A Report for the International Energy Agency Agreement on the Production and Utilization of Hydrogen Task 16, Hydrogen from Carbon-Containing Materials*.
- Munnik, P., De Jongh, P., & De Jong, K. (2015). Recent developments in the synthesis of supported catalysts. *Chemical Reviews*, 115(14), 6687-6718. American Chemical Society.
- Padilla, R., Priece, P., Lin, M., Lopez-Sanchez, J., & Zhong, Z. (2017). A versatile sonication-assisted deposition–reduction method for preparing supported metal catalysts for catalytic applications. *Ultrasonics Sonochemistry*, 35, 631-639.
- Perreault, F., Fonseca De Faria, A., & Elimelech, M. (2015). Environmental applications of graphene-based nanomaterials. *Chemical Society Reviews*, 44(16), 5861-5896.
- Rahman, M., Church, T., Variava, M., Harris, A., & Minett, A. (2014). Bimetallic Pt-Ni composites on ceria-doped alumina supports as catalysts in the aqueous-phase reforming of glycerol. *RSC Advances*.
- Rogalinski, T., Herrmann, S., & Brunner, G. (2005). Production of amino acids from bovine serum albumin by continuous sub-critical water hydrolysis. *Journal of Supercritical Fluids*, 36(1), 49-58.
- Stankovich, S., Dikin, D., Dommett, G., Kohlhaas, K., Zimney, E., Stach, E., . . . Ruoff, R. (2006). Graphene-based composite materials. *Nature*, 442(7100), 282-286.
- Stoller, M., Park, S., Yanwu, Z., An, J., & Ruoff, R. (2008). Graphene-Based ultracapacitors. *Nano Letters*, 8(10), 3498-3502.
- Suslick, K., McNamara, W., & Didenko, Y. (2001). Conditions during cavitation. *ACS Division of Environmental Chemistry, Preprints*, 41, págs. 976-977.
- Tsoncheva, T., Genova, I., Tsintsarski, B., Dimitrov, M., Paneva, D., Zheleva, Z., . . . Petrov, N. (2013). Transition metal modified activated carbons from biomass and coal treatment products as catalysts for methanol decomposition. *Reaction Kinetics, Mechanisms and Catalysis*, 110(2), 281-294.

US Department of energy. (s.f.). *Renewable Fuel Standard*. from <https://www.afdc.energy.gov/laws/RFS.html>

Valenzuela, M., Jones, C., & Agrawal, P. (2006). Batch aqueous-phase reforming of woody biomass. *Energy and Fuels*.

van Santen, R. (2010). Molecular Catalytic Kinetics Concepts. En R. van Santen, *Novel Concepts in Catalysis and Chemical Reactors*, 1-30. Weinheim, Germany: Wiley-VCH Verlag GmbH & Co. KGaA.

Wang, J., & Yin, Y. (2018). Fermentative hydrogen production using various biomass-based materials as feedstock. *Renewable and Sustainable Energy Reviews*, 92, 284-306.

Wiltowski, T., Mondal, K., Campen, A., Dasgupta, D., & Konieczny, A. (2008). Reaction swing approach for hydrogen production from carbonaceous fuels. *International Journal of Hydrogen Energy*, 33(1), 293-302.

Zhen, Z., & Zhu, H. (2017). Structure and properties of graphene. En Z. Zhen, & H. Zhu, *Graphene: Fabrication, Characterizations, Properties and Applications*, 1-12. Elsevier.

Zhou, Y., Chen, J., Wang, F., Sheng, Z., & Xia, X. (2010). A facile approach to the synthesis of highly electroactive Pt nanoparticles on graphene as an anode catalyst for direct methanol fuel cells. *Chemical Communications*, 46(32), 5951-5953.

CHAPTER 2. PREPARATION AND CHARACTERIZATION OF THE CATALYSTS

Abstract

In the present study, new reforming monometallic and bimetallic (Pt, Ni, W, Pt-Ni and Pt-W) graphene supported metal catalysts were developed by impregnation and ultrasound-assisted wet impregnation methods. Sequential reduction methods (first chemical reduction with NaBH_4 then thermal treatment) were applied to reduce metal precursors on the support. Characterizations of the catalysts were performed by transmission electron microscopy (TEM), X-ray diffraction (XRD), BET surface area measurement, infrared spectroscopy, Raman spectroscopy and inductively coupled plasma mass spectrometer (ICP-MS).

It was found that the size and distribution of metal particles on the graphene support were highly dependent on the metal type and the metal precursor used in the preparation of the catalysts. Ultrasound-assisted wet impregnation deposition method was the selected option to achieve 8 wt.% metal loading with smaller size and better dispersion of metal particles on the support. The sizes and distributions of Pt particles on graphene were found to be relatively small and uniform with narrow dispersion when the catalysts were prepared with PtCl_2 precursor. The catalysts prepared with inexpensive W showed better results compared to Ni based catalysts.

2.1 Introduction

Increasing demand, limited supply, and undesirable byproducts due to current methods indicates the need for the development of less expensive and more convenient, environmentally friendly ways for hydrogen production. Any sustainable alternatives that produce hydrogen in higher yield and richer composition could potentially reduce the cost of hydrogen production. In this matter, development of highly active catalysts for conversion of biomass to hydrogen is the most effective way for economically feasible hydrogen production.

The hydrothermal gasification technologies (sub- and supercritical water gasification and aqueous-phase reforming) have considerable economic, environmental, and technical advantages over other high demand energy conversion technologies. These processes are compatible with high water content feedstocks, such as biomass and gasification reactions take place at lower temperatures. However, lack of economically feasible, highly active, and stable catalysts for hydrothermal conversion of biomass-derived compounds to hydrogen is a main challenge that impedes upscaling of these technologies for hydrogen gas production.

Two important considerations must be made for precious metal catalysts such as platinum (Pt) which is able to convert biomass-derived compounds to hydrogen. The first is the economic use of precious metals and the probability of recovering and recycling them. The second is the necessity of using a support structure that provides the essential surface for the dispersion of the metal particles. However, the most noteworthy variables to take into consideration for this selection are, surface area, pore volume, pore size,

mechanical strength, resistance to attrition and thermal stability. (Meryemoğlu, Hasanoğlu, Kaya, Irmak, & Erbatur, 2014).

Platinum precious metal catalysts are used in the supported form on various supportive materials such as carbon, alumina, and silica. Among all these supports, carbon materials have been recognized as the most active supports for APR of biomass-derived compounds for hydrogen-rich gas production (Meryemoglu, Hesenov, Irmak, Atanur, & Erbatur, 2010). The interaction between active metal component and support plays an important role in the catalytic reactions. Therefore, catalytic properties of supported catalysts depend on the combination of the type of metal and supportive material.

The catalytic activity of metal particles on the support is highly dependent on the size and shape of the metal nanoparticle particles. Smaller metal nanoparticles affect the electronic density and increase the Fermi level energy, due to shortening of the Pt-Pt bonds (Roduner, 2006; Li, Li, Zang, Wang, & Zhang, 2014; Narayanan & El-Sayed, 2004). It was reported that decreasing Pt nanoparticle size of the catalyst leads to a lower coordination number of coordinated atoms that created active Pt sites by changing the electronic properties and the binding energies between Pt and reaction intermediates in water-gas shift reaction (Frenkel, Hills, & Nuzzo, 2001; Rodriguez, Liu, Hrbek, Evans, & Pérez, 2007).

Graphene can be an excellent catalyst support because of its stable structure and chemical inertness. These unique properties may improve catalyst stability and increase lifetime of the catalysts that could also reduce cost of the catalysts. Considering the high cost of precious metals there is a significant justification for developing innovative, and

effective catalysts for conversion of biomass compounds to hydrogen. Leaching of the metal particles from support is one of the main problems in this type of catalysts that causes decay of catalyst activity. The goal of this research is to develop new supported metal catalysts with novel properties using graphene as a promising catalyst support for hydrogen gas production from hydrothermal gasification of biomass.

The primary objectives are:

- I.** To develop Pt monometallic catalysts using different Pt precursors (H_2PtCl_6 , PtBr_2 , PtCl_2 and PtI_2) and graphene as supportive material.
- II.** To determine effect of sonication on the particle size and distribution of the Pt metal particles on the support.
- III.** To develop Ni and W monometallic and Pt-Ni and Pt-W bimetallic graphene supported catalysts.

2.2 Materials and Methods

2.2.1 Preparation of the catalysts

Incipient wetness impregnation method was used for preparation of graphene supported metal catalysts. All experiments were performed with 0.8 g graphene and appropriate amount of metal precursor to deposit 8 wt% metal on the support. Graphene supportive material (Acros Organics, 2-10 nm) and metal precursor salt were mixed in the 25 ml water and magnetically stirred for 20 min at room temperature. The mixture was sonicated at 10 kHz for 10 min using a sonication prob (Q55, QSonica). After sonication, the mixture was magnetically stirred and heated until dryness at 70 °C. 10 ml of 0.30 M NaBH_4 was added drop by drop to reduce metals on the support while stirring.

The mixture was centrifuged; liquid and solid were separated. Solid fraction was mixed with 10 ml of water and centrifuged again. The liquid fractions were combined and kept for metal analysis. The solid fraction (catalyst) was dried at 80 °C. The dry catalyst was put in a ceramic boat crucible that were placed in a quartz tube within a tube furnace (B400/410, Nabertherm) and thermally reduced under N₂ flow (100 ml/min) for 6 h at 300 °C. The metal composition of bimetallic catalysts (Pt-Ni and Pt-W) were 4 wt% for each metal (8 wt% of total metals). Table 2.1 shows the list of metal precursors that was used for the preparation of the catalysts.

Table 2.1. Metal precursors used for the preparation of the catalysts.

Precursor	Metal deposited on graphene
Hexachloroplatinic (IV) acid hexahydrate (H ₂ PtCl ₆ .6H ₂ O)	Pt
Platinum (II) bromide (PtBr ₂)	Pt
Platinum (II) chloride (PtCl ₂)	Pt
Platinum (II) iodide (PtI ₂)	Pt
Nickel (II) chloride (NiCl ₂)	Ni
Ammonium tungstate pentahydrate (NH ₄) ₁₀ W ₁₂ O ₄₁ ·5H ₂ O	W

Hexachloroplatinic (IV) acid and nickel (II) chloride	Pt-Ni (4 wt% for each metal)
Hexachloroplatinic (IV) acid and ammonium tungstate pentahydrate	Pt-W (4 wt% for each metal)

2.2.2 Characterization of the catalysts

The transmission electron microscopy images of the catalysts were performed by a FEI Tecnai Osiris 200 kV S/TEM (ThermoFisher Scientific). Quantifoil 200# 2UM copper grid coated with a holey carbon film (Electron Microscopy Sciences) was used as specimens for TEM examination. Particle size distribution from TEM images were determined by ImageJ software. X-Ray diffraction analysis of the catalyst samples were performed with Rigaku SmartLab Diffractometer using Cu K α radiation at $\sim 1.54 \text{ \AA}$. The specimen was scanned from $2\theta=5-85^\circ$. Amount of Pt deposited on graphene were determined by inductively coupled plasma mass spectrometer (ICP-MS) analysis using a Thermo Scientific iCAP RQ ICP-MS. This analysis was applied to the liquid solution that was collected after centrifugation of the mixture that was treated with NaBH $_4$ and the washed with water. Infrared spectra of graphene were performed on Nicolet Avatar 380 FT-IR with Smart Performer ATR accessory with a diamond crystal. A Thermo Scientific DXR Raman microscope with a 532 nm excitation laser was used for Raman Spectroscopy. Specific surface area of the catalysts and support were determined by nitrogen adsorption and the data collected were analyzed based on Brunauer-Emmett-Teller (BET) theory (Thommes, Köhn, & Früba, 2000) using a Micromeritics ASAP 2020 Surface Area and Porosity Analyzer.

2.3 Results and Discussion

2.3.1 Characterization of graphene before and after being used as a catalyst support

Materials should be chemically and thermochemically stable to be used as catalyst support. Graphene is known to have great stability; however, it needs to be tested if the catalysts preparation process caused some changes in its structure. FTIR and Raman spectroscopy were used to determine these structural changes in graphene after they were exposed to several steps during catalysts preparation process such as sonication, reduction treatment with NaBH_4 and thermal treatment under nitrogen. The FTIR spectrum shows the characteristic peaks of C=C of graphene materials in the range of $1340\text{--}1700\text{ cm}^{-1}$. The peaks at 1060 cm^{-1} and 1617 cm^{-1} were due to C-H and C=C, respectively (Figure 2.1). The spectra show that the graphene samples do not contain hydroxyl groups (--OH , 3350 cm^{-1}), carboxyl groups (COOH , 1740 cm^{-1}) or carbonyl groups (C=O , 1660 cm^{-1}) that are indication that no oxidation occurred during the treatment. There are some negligible minor changes in the appearance of some bands but, in general, the treatment(s) (sonication, reduction treatment with NaBH_4 and thermal treatment under nitrogen) did not cause considerable changes in the graphene structure. If graphene was oxidized, graphene oxide type of structure was expected (Figure 2.2). This was confirmed by Raman spectroscopy as well (Figure 2.3).

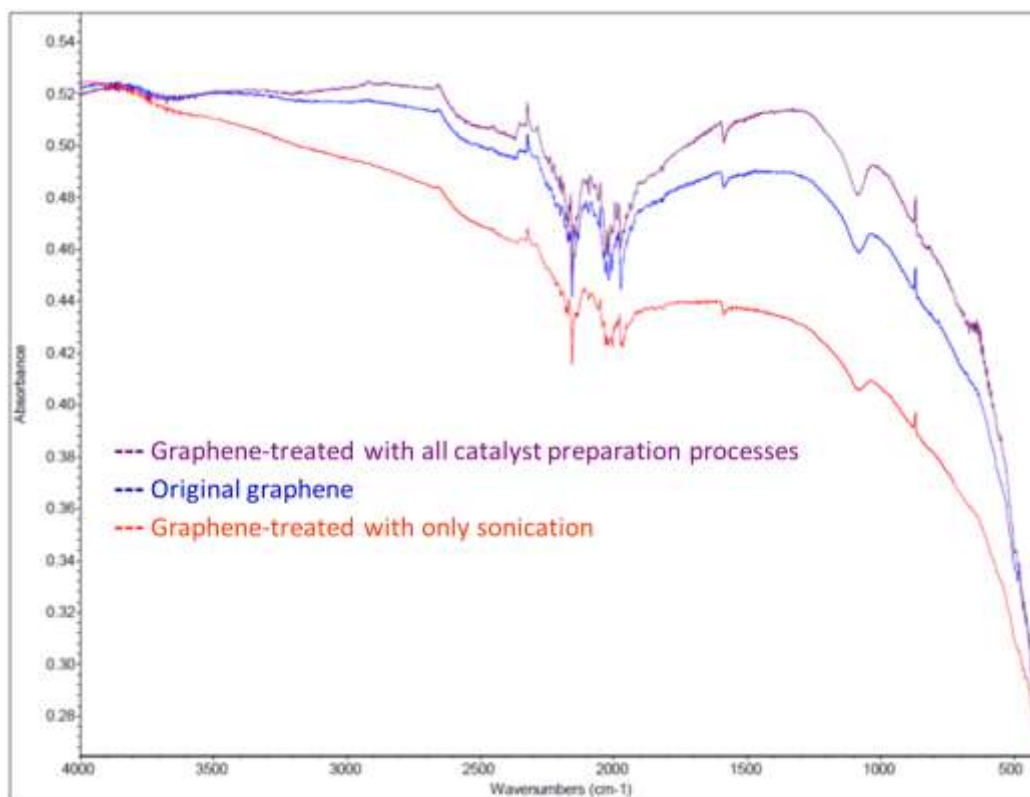


Figure 2.1. Infrared spectra of graphene samples.

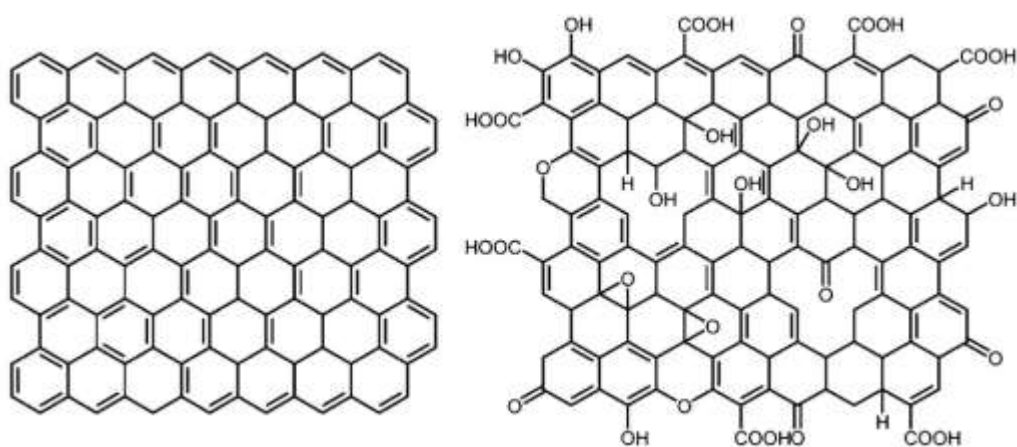


Figure 2.2. Structures of graphene and graphene oxide (Perreault, Fonseca De Faria, & Elimelech, 2015).

Based on the Raman spectra, there is a sharp G-band peak ($\sim 1600\text{ cm}^{-1}$) being larger than splitted 2D-band peak ($\sim 2700\text{ cm}^{-1}$). The G-band refers to the graphene (sp^2) and 2D-band is the indication of the stacking order of graphene layers (Ferrari, 2007; Saito, Hofmann, Dresselhaus, Jorio, & Dresselhaus, 2011).

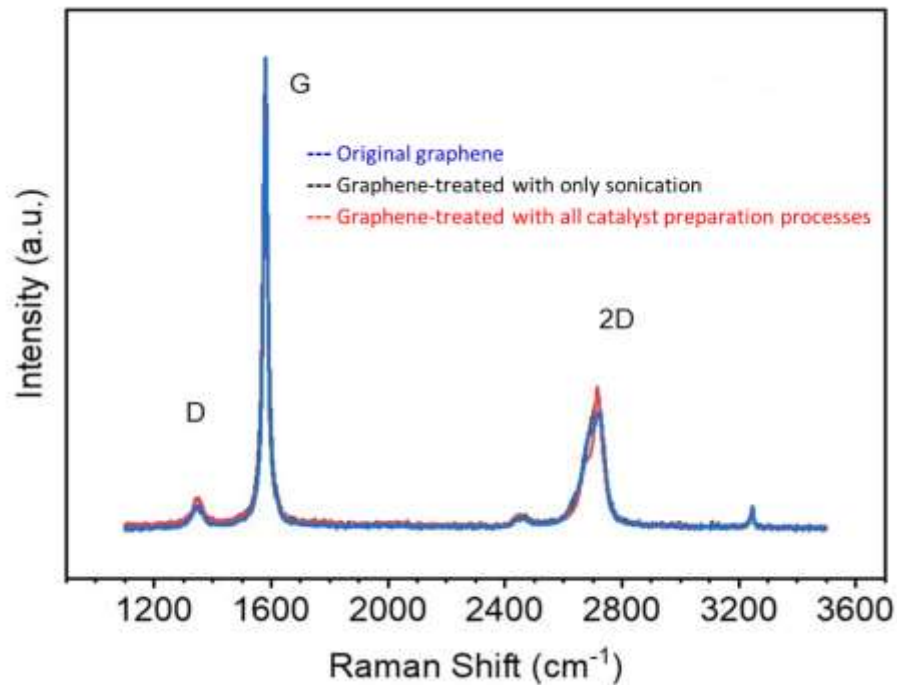


Figure 2.3. Raman spectra of graphene samples.

There is also a clear D-band peak (1350 cm^{-1}) which shows disorder structure of graphene (i.e. defects in graphene). This exists in the original graphene as well as treated graphene samples (Figure 2.3). Overall, there is no clear difference between the three graphene samples that indicate graphene preserves its structure after being exposed to all steps used in catalyst preparation.

2.3.2 Amounts of metals deposited on graphene

All catalysts were prepared to contain 8 wt.% metal particles on the graphene support. The actual metal loadings of supported metal catalysts were determined by ICP-MS analysis and given in Table 2.2. It was found that 8 wt.% of metal loading was achieved in all catalysts prepared using different Pt precursors when ultrasound-assisted wet impregnation deposition method was used. With only one exception, there were no significant differences ($P>0.05$) in the catalysts prepared by sonication and non-sonication treatments to achieve 8 wt.% Pt deposition on the graphene support. However, there was significant difference ($P<0.05$) in the catalyst prepared with PtCl_2 precursor. In this catalyst, Pt% on graphene was observed to be lower when ultrasonication was not applied for the preparation of this catalyst.

Table 2.2. Comparison of theoretical and actual Pt amount deposited on the support*

Catalyst	Theoretical Pt% deposited	Actual Pt% deposited
H_2PtCl_6	8.15 ± 0.09	8.10 ± 0.11 a
S- H_2PtCl_6	7.96 ± 0.02	8.09 ± 0.04 a
PtBr_2	8.04 ± 0.12	8.02 ± 0.11 a
S- PtBr_2	8.01 ± 0.13	8.11 ± 0.23 a
PtCl_2	7.95 ± 0.10	8.15 ± 0.08 a
S- PtCl_2	8.06 ± 0.07	8.09 ± 0.04 a
PtI_2	8.08 ± 0.07	7.12 ± 0.11 a
S- PtI_2	8.07 ± 0.01	8.06 ± 0.01 b

*Theoretical Pt% deposited: Calculated based on precursor amount used in preparation of the catalyst. Actual Pt% deposited: Determined by ICP-MS analysis. Mean \pm standard deviation from three replications.

Values followed by same letters within sonicated and non-sonicated catalysts are not significantly different ($P > 0.05$).

Table 2.3 shows comparison of metal particles deposited on graphene in monometallic Ni and W and bimetallic Pt-Ni and Pt-W compositions. All these catalysts were prepared by ultrasound-assisted wet impregnation deposition method. As can be seen in the table, 4 wt.% of metal deposition for each metal in bimetallic catalysts (total of 8 wt.%) and 8 wt.% metal deposition in monometallic catalysts were successfully achieved.

Table 2.3. Comparison of theoretical and actual metal amounts deposited on the graphene by ultrasound-assisted wet impregnation method*

Catalyst	Theoretical Pt% deposited	Actual Pt% deposited
Pt in Pt-Ni	3.99 ± 0.02	3.98 ± 0.01
Pt in Pt-W	3.98 ± 0.02	3.97 ± 0.02
Ni	8.04 ± 0.02	8.01 ± 0.03
Ni in Pt-Ni	4.06 ± 0.10	4.01 ± 0.01
W	7.94 ± 0.09	7.93 ± 0.12
W in Pt-W	3.95 ± 0.06	4.02 ± 0.13

*Theoretical Pt% deposited: Calculated based on precursor amount used in preparation of the catalyst. Actual Pt% deposited: Determined by ICP-MS analysis.

2.3.3 TEM images

The activity of the catalyst is strongly related to size and distribution of the metal particles on the support. Nano sizes with narrow distribution and well-distributed metal particles are known to be ideal (Yu, et al., 2013; Kumarasinghe, et al., 2013).

The transmission electron microscopy (TEM) images of sonicated and non-sonicated catalysts prepared using PtI_2 precursor were presented in Figure 2.4. The particle size distributions found from these images were also included in Figure 2.4. Spherical and rod shape particles are seen in the TEM images of non-sonicated PtI_2 catalyst. These different shaped particles were confirmed to be Pt metal particles by Energy dispersive spectroscopy (EDS) that was coupled with the TEM instrument used. In EDS, X-ray energies are used to identify the elements present in the sample. X-rays emitted from a specific metal are used to identify the metal based on energy released. As can be seen in Figure 2.4, copper (Cu) was also observed in EDS spectra. The specimens (TEM grids) used in TEM measurement had Cu which was detected in the samples. Use of sonication in preparation of PtI_2 catalyst reduced formation of rod type particles and resulted in deposition of Pt as smaller sized particles with better dispersion on the support.

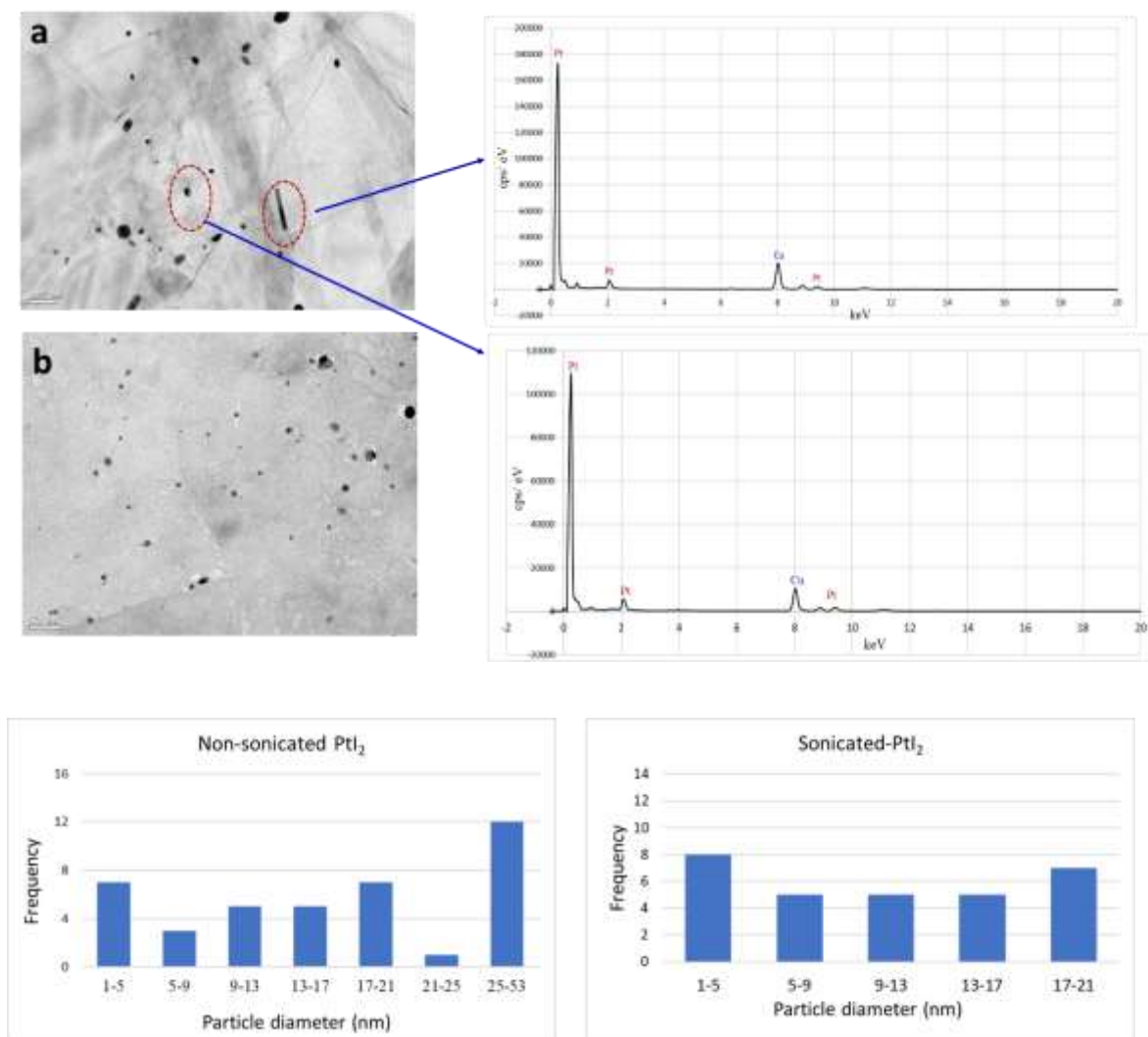


Figure 2.4. TEM images, EDS spectra and particle size distributions of non-sonicated (a) and sonicated (b) catalysts prepared using PtI_2 precursor.

Figure 2.5 shows comparison of sonicated catalysts prepared using PtCl_2 , PtBr_2 and H_2PtCl_6 precursors. PtCl_2 precursor found to be best precursor to prepare Pt catalyst in terms of size of metal particles and their distribution. The sizes and distributions of Pt particles on graphene were relatively small (1-9 nm) and they were uniform with narrow dispersion compared to the catalysts prepared with other precursors.

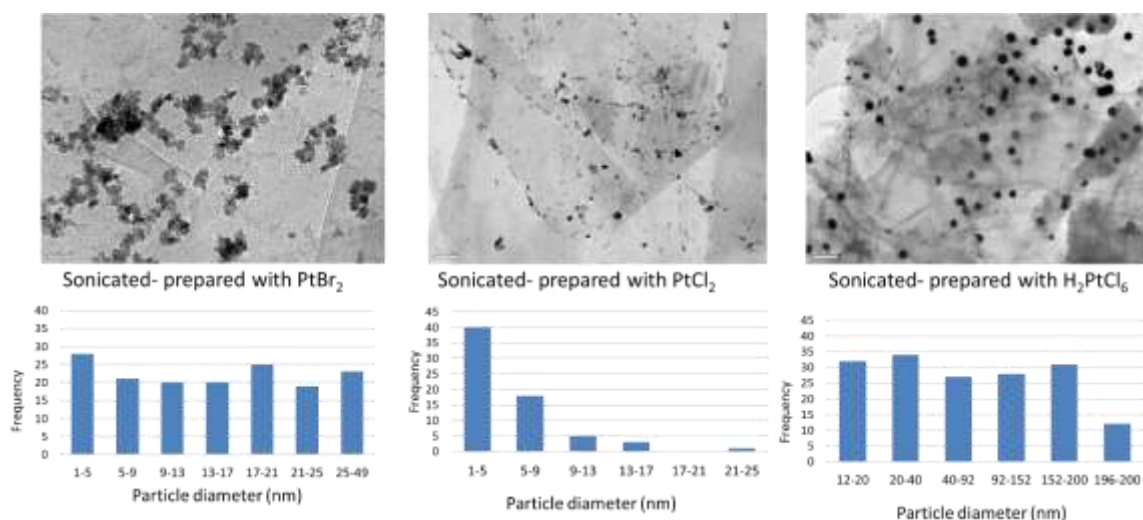


Figure 2.5. TEM images and particle size distributions of the catalysts prepared with different platinum precursors by application of sonication.

Deposition of Ni on graphene resulted in larger particles with wide dispersion compared to W (Figure 2.6). The particle size of the metal particles became even larger when the catalysts were prepared in bimetallic composition with combination of Pt.

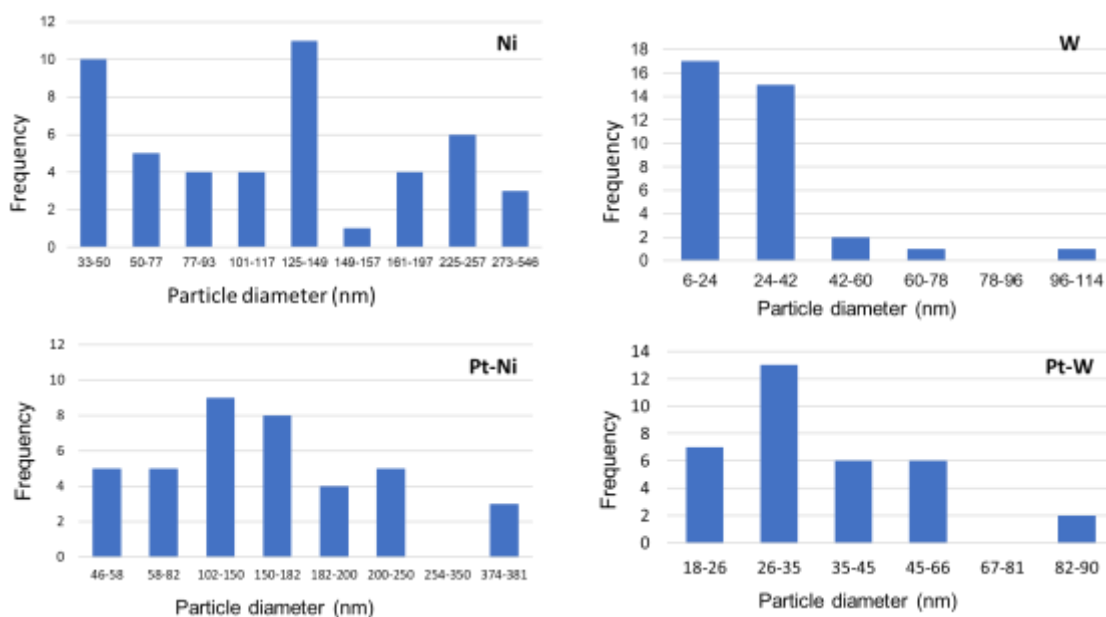


Figure 2.6. TEM images and particle size distributions of the catalysts prepared with different metals.

2.3.4. XRD of the catalysts

The XRD spectra of the catalysts were measured in a range of 2θ from 5° to 85° (Figure 2.7). The peaks at 2θ values of 40.1° , 46.8° and 67.7° are the characteristic peaks of face-centered-cubic (fcc) crystalline structures of Pt. These 2θ values are corresponding to the planes of (111), (200) and (220), respectively (Yang, Coutanceau, Léger, Alonso-Vante, & Lamy, 2005). These results indicate that all Pt precursors reduced to metallic form by the formation of face centered cubic Pt. XRD patterns of all catalysts were similar; the characteristic peaks were observed at same 2θ . However, the intensities of these peaks were different which indicates particle size of the Pt metal particles were different.

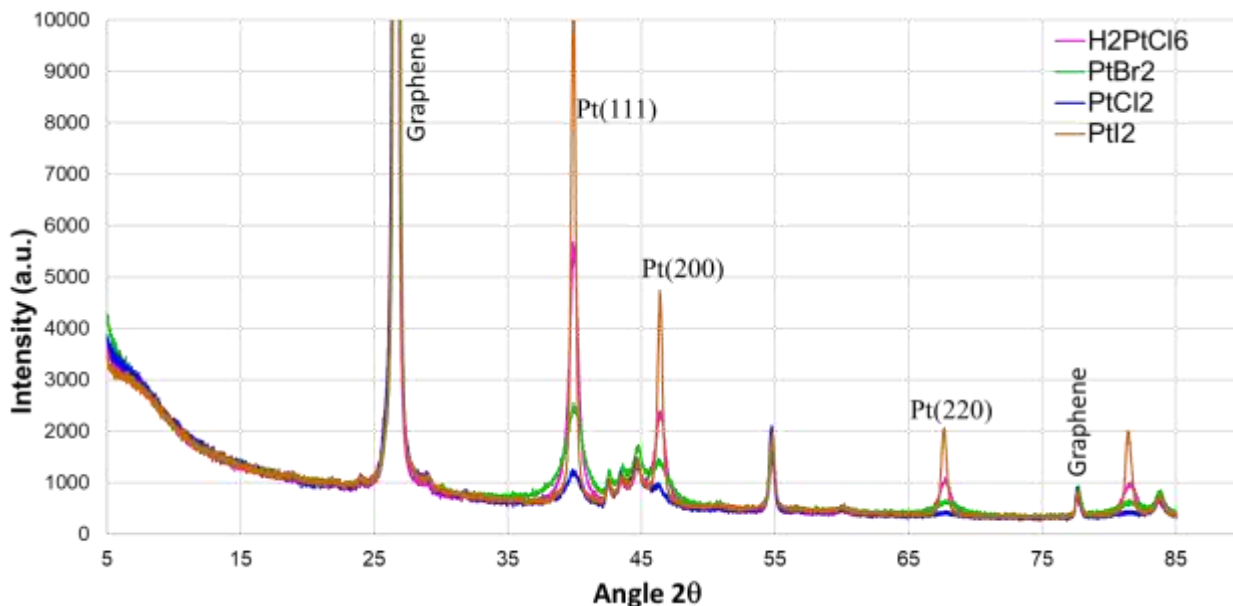


Figure 2.7. XRD patterns of the catalysts prepared with different Pt precursors.

As can be seen in Figure 2.8, the Pt(111) and Pt(200) peaks in Pt-Ni slight shift and Pt(220) is not seen in the XRD pattern. The reason of these changes is that nickel could completely or partially become alloyed with platinum and participate into the fcc structure of Pt (Lin, Cui, Yen, & Wai, 2005). It was reported in the literature that XRD patterns of the Ni and Ni-Pt samples were hardly distinguishable, because of dispersing Pt in Ni-Pt catalyst (Gawande, et al., 2012). Same thing could be true for W in Pt-W catalyst.

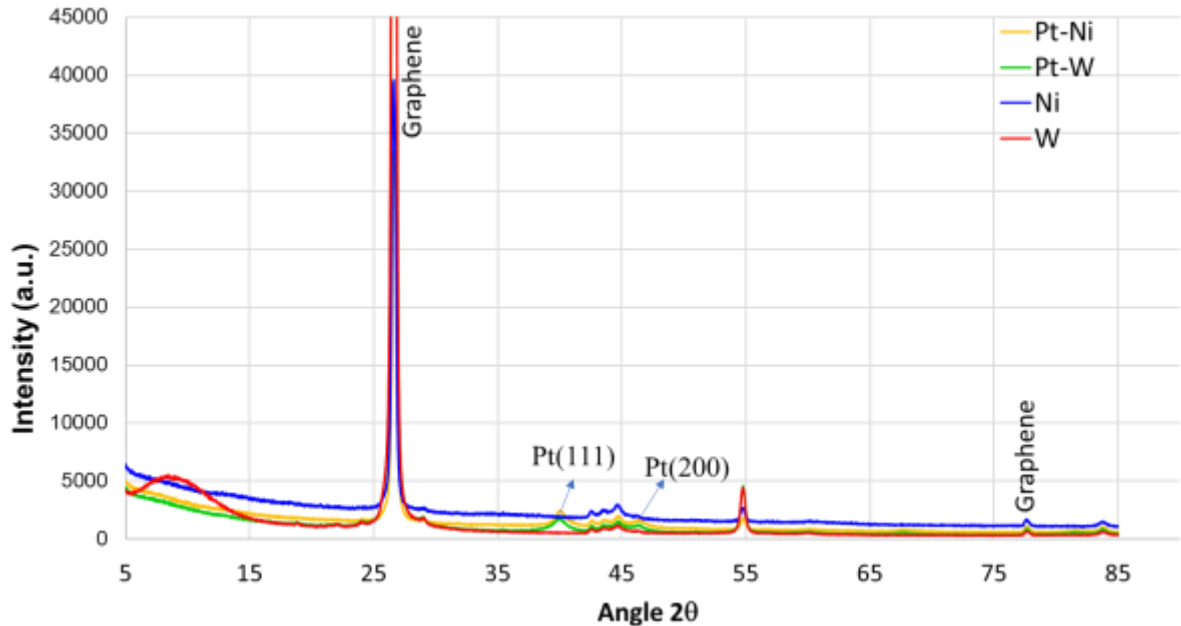


Figure 2.8. XRD patterns of the catalysts prepared with different metals.

The characteristic (111), (200) and (220) planes of Ni phase are supposed to be seen at $2\theta = 44.4^\circ$, 51.7° and 76.5° in XRD patterns of Ni monometallic catalyst. Deposition only 8 wt% Ni on the support did not show an observable degree of crystallinity in the XRD

pattern. In literature, the intensity of 20 wt% Ni deposited on Al₂O₃ support was found to be ~150 while no peak was observed in 20 wt% Ni deposited on SiO₂ support. In addition, the XRD diffractograms of 2.5 wt% Ni/SiO₂ and Ni/Al₂O₃ catalysts showed no crystalline Ni because of the low amount of Ni loading was beyond the detection limit of the XRD technique (Abd El Maksod & Saleh, 2010). Same thing could be considered for W monometallic catalyst since W peak was not detected in the XRD spectrum. It was reported in the literature that when W loading is higher than ca. 20 wt% the peaks can be detectable by XRD (MaCcarrone, et al., 2016).

2.3.5 Surface area and pore volume comparisons of the catalysts

Surface area is an important parameter in understanding and evaluating catalytic activity of the catalysts. Graphene has a high theoretical surface area (2,630 m² /g). However, large extent of van der Waals interactions between surfaces lead to graphene sheets to stack on top of each other. Surface area between graphene layers becomes inaccessible depending on degree of stacking. As can be seen in Table 2.4, the surface area of graphene support was determined to be low, which is attributed to extensive stacking between graphene layers. When all the treatments were applied to graphene support without using any metal precursor, the surface area was doubled. Use of different Pt precursors did not increase the surface area to the value that can be comparable with theoretical surface area. These results are in accordance with the Raman spectroscopy results in which it was found the graphene used in this study had monolayer graphene structure. Pore volume of the catalysts were found to be higher than original-untreated graphene. It is interesting to point out that the catalyst prepared with PtBr₂ had considerably higher pore volume than other catalysts.

Table 2.4. Comparison surface areas and pore volumes of the catalysts prepared with different Pt precursors

Catalyst	BET surface area (m²/g)	Pore volume (cm³/g)
Graphene	10.82	0.068
Graphene-treated	20.98	0.091
H ₂ PtCl ₆ /Graphene	17.59	0.098
PtBr ₂ /Graphene	21.85	0.132
PtCl ₂ /Graphene	11.94	0.077
PtI ₂ /Graphene	12.55	0.076

Similar results were found when the catalysts were prepared with different metals (Table 2.5). In monometallic catalysts surface area was decreased as the size of metal increased. The covalent radius of the metals in the literature are given as follows: W (193 pm); Pt (177 pm) and Ni (149 pm). The values are in picometres (pm or 1×10^{-12} m) and atomic radii computed from theoretical models (Clementi, Raimondi, & Reinhardt, 1967). The distance between the nuclei of two identical atoms (e.g. Pt-Pt; W-W or Ni-Ni) bonded together is measured and given as atomic radii. Ni atom has lower atomic radius therefore it blocks less surface on graphene and the surface area of the catalyst prepared with Ni had slightly higher surface area compared to Pt and W.

Table 2.5. Comparison of surface areas and pore volumes of the catalysts prepared with different metals

Catalyst	BET surface area (m²/g)	Pore volume (cm³/g)
Pt/Graphene	17.59	0.098
Ni/Graphene	20.71	0.085
W/Graphene	15.58	0.087
Pt-Ni/Graphene	17.92	0.095
Pt-W/Graphene	14.31	0.077

2.4 Conclusion

The graphene support did not change its properties when exposed to the catalyst preparation treatments. Total of 8 wt.% of metal loading was successfully achieved when ultrasound-assisted wet impregnation deposition method was used. When catalyst was prepared using PtCl₂ precursor, the sizes and distributions of Pt particles on graphene were relatively small (1-9 nm) and uniform with narrow dispersion compared to the catalysts prepared with PtI₂, PtBr₂ and H₂PtCl₂ precursors. Deposition of W particles on graphene exhibited better results than Ni catalysts in terms of metal particle size and distribution.

References

- Abd El Maksod, I., & Saleh, T. (2010). The use of nano supported nickel catalyst in reduction of -nitrophenol using hydrazine as hydrogen donor. *Green Chemistry Letters and Reviews*, 3(2), 127-134.
- Clementi, E., Raimondi, D., & Reinhardt, W. (1967). Atomic screening constants from SCF functions. II. Atoms with 37 to 86 electrons. *The Journal of Chemical Physics*, 47(4), 1300-1307.
- Ferrari, A. (2007). Raman spectroscopy of graphene and graphite: Disorder, electron-phonon coupling, doping and nonadiabatic effects. *Solid State Communications*, 143(1-2), 47-57.
- Frenkel, A., Hills, C., & Nuzzo, R. (2001). A view from the inside: Complexity in the atomic scale ordering of supported metal nanoparticles. *Journal of Physical Chemistry B*, 105(51), 12689-12703.
- Gawande, M., Rathi, A., Branco, P., Nogueira, I., Velhinho, A., Shrikhande, J., . . . Teodoro, O. (2012). Regio- and chemoselective reduction of nitroarenes and carbonyl compounds over recyclable magnetic ferrite-nickel nanoparticles (Fe 3O 4-Ni) by using glycerol as a hydrogen source. *Chemistry - A European Journal*, 18(40), 12628-12632.
- Kumarasinghe, A., Samaranayake, L., Bondino, F., Magnano, E., Kottegoda, N., Carlino, E., . . . Amaratunga, G. (2013). Self-assembled multilayer graphene oxide membrane and carbon nanotubes synthesized using a rare form of natural graphite. *Journal of Physical Chemistry C*, 117(18), 9507-9519.
- Li, X., Li, G., Zang, W., Wang, L., & Zhang, X. (2014). Catalytic activity of shaped platinum nanoparticles for hydrogenation: A kinetic study. *Catalysis Science and Technology*, 4(9), 3290-3297.
- Lin, Y., Cui, X., Yen, C., & Wai, C. (2005). PtRu/carbon nanotube nanocomposite synthesized in supercritical fluid: A novel electrocatalyst for direct methanol fuel cells. *Langmuir*, 21(24), 11474-11479.

- MaCarrone, M., Lederhos, C., Betti, C., Carrara, N., Yori, J., Pascual, F., . . . Quiroga, M. (2016). Nanoparticles of tungsten as low-cost monometallic catalyst for selective hydrogenation of 3-Hexyne. *Quimica Nova*, 39(1), 1-8.
- Meryemoğlu, B., Hasanoğlu, A., Kaya, B., Irmak, S., & Erbatur, O. (2014). Hydrogen production from aqueous-phase reforming of sorghum biomass: An application of the response surface methodology. *Renewable Energy*.
- Meryemoglu, B., Hesenov, A., Irmak, S., Atanur, O., & Erbatur, O. (2010). Aqueous-phase reforming of biomass using various types of supported precious metal and raney-nickel catalysts for hydrogen production. *International Journal of Hydrogen Energy*.
- Narayanan, R., & El-Sayed, M. (2004). Shape-dependent catalytic activity of platinum nanoparticles in colloidal solution. *Nano Letters*, 4(7), 1343-1348.
- Perreault, F., Fonseca De Faria, A., & Elimelech, M. (2015). Environmental applications of graphene-based nanomaterials. *Chemical Society Reviews*, 44(16), 5861-5896.
- Rodriguez, J., Liu, P., Hrbek, J., Evans, J., & Pérez, M. (2007). Water gas shift reaction on Cu and Au nanoparticles supported on CeO₂(111) and ZnO(0001): Intrinsic activity and importance of support interactions. *Angewandte Chemie - International Edition*, 46(8), 1329-1332.
- Roduner, E. (2006). Size matters: Why nanomaterials are different. *Chemical Society Reviews*, 35(7), 583-592.
- Saito, R., Hofmann, M., Dresselhaus, G., Jorio, A., & Dresselhaus, M. (2011). Raman spectroscopy of graphene and carbon nanotubes. *Advances in Physics*, 60(3), 413-550.
- Thommes, M., Köhn, R., & Früba, M. (2000). Sorption and pore condensation behavior of nitrogen, argon, and krypton in mesoporous MCM-48 silica materials. *Journal of Physical Chemistry B*, 104(33), 7932-7943.
- Yang, H., Coutanceau, C., Léger, J., Alonso-Vante, N., & Lamy, C. (2005). Methanol tolerant oxygen reduction on carbon-supported Pt-Ni alloy nanoparticles. *Journal of Electroanalytical Chemistry*, 576(2), 305-313.

Yu, X., Huo, Y., Yang, J., Chang, S., Ma, Y., & Huang, W. (2013). Reduced graphene oxide supported Au nanoparticles as an efficient catalyst for aerobic oxidation of benzyl alcohol. *Applied Surface Science*, 280, 450-455.

CHAPTER 3. EVALUATION OF THE CATALYSTS FOR CONVERSION OF BIOMASS COMPOUNDS TO HYDROGEN GAS BY APR

Abstract

The present study was designed to evaluate graphene supported metal catalysts that were prepared using different Pt precursors ($\text{H}_2\text{PtCl}_6 \cdot 6\text{H}_2\text{O}$, PtBr_2 , PtCl_2 , and PtI_2) and different metals in monometallic (Pt, Ni and W) and bimetallic (Pt-Ni and Pt-W) combinations for hydrothermal gasification of biomass compounds. The catalysts were prepared by wet impregnation and ultrasound-assisted wet impregnation for comparison. The gasification was performed by aqueous-phase reforming (APR) as a low temperature hydrothermal gasification technology. Glucose, a simple biomass-derived compound, was used as substrate in the APR process.

The Pt precursors evaluated in the study produced similar amounts of hydrogen gas if the catalysts were prepared under ultrasonication. Catalytic activity of monometallic Ni and W catalyst significantly increased when these metals were used in combination with Pt by replacing half amount of Pt with Ni or W. These findings indicate that Pt-W/graphene and Pt-Ni/graphene catalysts could be promising catalysts to produce hydrogen in higher yield and richer composition by hydrothermal gasification of biomass-derived compounds.

3.1 Introduction

Aqueous-phase reforming (APR) is a process that operates under low temperatures, between 200 and 250 °C, using high pressures ranging from 15 to 50 bar. This temperature range is considerably lower than other reforming methods, such as alkane steam reforming, which operates at about 620 °C (Meryemoğlu, Hasanoğlu, Kaya, Irmak, & Erbatur, 2014). APR produces hydrogen and light alkanes, and the reactants remain in a liquid phase, thus, avoiding the need of evaporating the liquid and reducing the energy consumption. Working at low temperatures, thermodynamically favors the production of hydrogen with low carbon monoxide concentration. The selectivity of the catalyst is of uttermost importance. The catalyst used in APR should break the C-C bonds and advance the CO consumption efficiently during the water-gas shift reaction to produce H₂ and CO₂. Neither the breaking of the C-O bond nor the hydrogenation of CO or CO₂ should be incentivized by the catalyst (Davda & Dumesic, 2004).

There is evidence that hydrocarbon with C:O ratios of 1:1 have a very high H₂ conversion rate, nonetheless, most of the CO and H₂ produced react almost immediately to produce alkanes and water. This shows the importance of the catalyst in APR process to increase hydrogen gas production and selectivity (Cortright, Davda, & Dumesic, 2002).

Development of robust catalysts that are stable and selective under aqueous-phase reaction conditions would advance the utility of APR as well as other hydrothermal gasification technologies for hydrogen gas production. Raney nickel and platinum-based catalysts have been known to be most active catalysts for hydrogen gas production by hydrothermal processes (Meryemoglu, Hesenov, Irmak, Atanur, & Erbatur, 2010; Davda, Shabaker, Huber, Cortright, & Dumesic, 2003). Although activity of Raney nickel

catalysts is better than precious metals, use of these catalysts for hydrothermal gasification have several drawbacks including the following:

- Raney nickel catalysts can spontaneously ignite when exposed to air because of containing significant amounts of hydrogen gas. For this reason, raney nickel catalysts are kept in water or in a suitable solvent such as ethanol, cyclohexane, dioxane, etc. and handled under an inert atmosphere.
- Deactivation of Raney nickel in hydrothermal conditions is a major problem. Surface area and metal particle size measurement showed that nickel metal particle size in Raney-Ni catalysts became larger and surface area was considerable reduced after deactivation. The oxidation of Raney-Ni surface is the major cause of its deactivation. Therefore, reaction condition should be kept reductive as possible to preserve metallic state of Raney-Ni and to maintain its activity (Nguyen, Lu, Kobayashi, Ishikawa, & Komiyama, 2014).
- Nickel preserves its metallic state under steam reaction medium (Nguyen, Lu, Kobayashi, Ishikawa, & Komiyama, 2014). If carbon content of the reaction medium is high, stability of the nickel catalyst decreases. This is a big challenge for any hydrothermal condition in which organic-rich solutions/materials are used as feeds.

Platinum precious metal catalysts are used in the supported form on various supportive materials such as carbon, alumina and silica in the many processes. Efforts have been made so far significantly improved catalytic activity of these catalysts towards hydrogen, however, they are still not comparable with Raney nickel catalysts in terms of hydrogen production yield. The main reasons for activity loss of supported precious metal catalysts are aggregation or poisoning of metal particles in reaction medium or coke deposition on

active surfaces of the catalysts (Ren, et al., 2007). Leaching of the metal particles from support is another problem that causes decay of catalyst activity.

Increasing the catalytic activity and stability of the catalysts is a challenge for high yielding hydrogen gas production. The goal of the present study is to develop economically feasible and highly active catalysts for hydrothermal conversion of biomass-derived compounds to hydrogen.

The primary objectives of this study are:

- I.** To determine activity of Pt-based catalysts that were prepared from different of Pt precursors and graphene as supportive material for hydrogen gas production by APR of biomass compound, glucose.
- II.** To compare activity of the catalysts that were prepared by sonication and non-sonication wet impregnation process.
- III.** To evaluate activity of graphene supported Pt, Ni, W, Pt-Ni and Pt-W catalysts for high yielding-hydrogen gas production by APR.

3.2 Materials and Methods

3.2.1 Catalysts

The graphene (Acros Organics, 2-10 nm) supported metal catalysts were prepared by the impregnation method. The mixture of metal salt(s) (total of 8wt% metal) and support (0.8 g) in 25 mL water were magnetically stirred at room temperature for 20 min. Then, the mixture was sonicated for 10 min (10 kHz, Q55 QSonica) while magnetically stirring. The resulting slurry were dried at 70°C to remove the solvent. The metal precursors on the support were reduced by using a reducing agent, NaBH₄ (10 ml

of 0.3 M NaBH₄). The solid fraction was collected by centrifugation at 3500 rpm and later filtered. The solid was washed with 10 ml of water and collected with centrifugation again before drying 80°C. Then, it was thermally reduced under N₂ flow (10 ml/min) for 6 h at 300 °C by replacing the samples on alumina process tube within a tube furnace (B400/410, Nabertherm).

The supported metal catalysts were prepared with various Pt precursors:

hexachloroplatinic (IV) acid hexahydrate, platinum (II) bromide, platinum (II) chloride and platinum (II) iodide. The inexpensive metals Ni and W were also deposited on graphene support in monometallic (8% metal) and bimetallic compositions (4% Pt and 4% other metal). Hexachloroplatinic (IV) acid hexahydrate, nickel (II) chloride and ammonium tungstate pentahydrate were used as precursors in preparation of bimetallic catalysts.

Characterization of the catalysts were performed by transmission electron microscopy (TEM), X-ray diffraction (XRD), Brunauer–Emmett–Teller (BET) surface area measurement, infrared spectroscopy and inductively coupled plasma mass spectrometry (ICP-MS).

3.2.2 Evaluation of the catalysts by APR

Hydrogen gas production activity of the catalysts were evaluated by APR of glucose solution (150 mg/L). The gasification experiments (APR) were carried out in a Parr 4520 benchtop 600 mL stainless steel reactor equipped with magnetic drive stirrer and a temperature control system (Parr Instrument Co., Moline, IL). 350 mL glucose solution and 0.1750 g catalysts were placed in the reactor. The air in the sealed reactor was purged with high purity argon (6895 kPa) gas before gasification process.

Gasification was performed at 250°C for 90 min at 4136 psi. After cooling down the reactor to room temperature, the gas mixture produced was collected into a gas burette that was filled with water to determine the volume. The contents and composition of the gas mixture were determined by a gas chromatograph equipped with a thermal conductivity detector (TCD) (Thermo Scientific Trace 1300). Argon was used as the carrier gas. The standard gas mixture used was composed of the following gases as mole percentages: 2.02 acetylene, 4.21 ethylene, 4.06 ethane, 4.99 methane, 15.1 carbon monoxide, 20.2 carbon dioxide and balance amount of hydrogen (49.42) (Matheson, Sioux City, IA). Carboxen 1010 plot fused silica capillary (30 m x 0.53 mm) column (Supelco, Bellefonte, PA) was used in gas analysis. The 500 μ L gas mixture and standard was injected into GC in split (1:3) injection mode. The GC was programmed at 40°C for 3 min, increased to 230°C with 20°C/min heating rate and held at 230°C for 10 min. Inlet and detector temperatures were 230°C and filament was at 360°C. The column gas flow and reference gas flow were 40 mL/min and 5 mL/min, respectively.

3.2.3 Statistics analysis

All catalysts preparation and gasification experiments runs were carried out in triplicates. Samples from each gasification experiment were analyzed by at least three injections in GC. The means of two injections per replication were used in the statistical analysis. Statistical analyses (Tukey's HSD multiple comparison test or pair t-test two samples for means) were conducted at the 5% significance level ($\alpha=0.05$).

3.3 Results and Discussion

3.3.1 Effect of Pt precursor types on the activity of Pt-graphene catalyst

The performance of the metal catalysts for various reactions can be different when different precursors are used in preparation of the catalysts (Borges, et al., 2019; Geng, et al., 2019). Same thing could be true for hydrothermal gasification reactions of biomass-derived compounds where different types of platinum precursors could exhibit different activity. The experimental results of gasification of glucose by APR in presence of Pt/graphene catalysts prepared using four different Pt precursors without application of sonication during impregnation process were presented in Table 3.1. PtCl_2 catalyst produced significantly higher ($P < 0.05$) gas mixture than H_2PtCl_6 and PtI_2 based catalysts while PtCl_2 and PtBr_2 catalysts produced similar ($P > 0.05$) amount of gas mixtures. PtCl_2 produced higher hydrogen gas than H_2PtCl_6 and PtI_2 while PtI_2 produced significantly lower hydrogen gas than PtCl_2 and PtBr_2 catalysts. However, there were no statistically significant differences ($P > 0.05$) in the contents of CO and CO_2 gases except PtI_2 catalyst in which CO and CO_2 amounts were found to be the highest (Table 3.1). Hydrogen production yield was found to be 4.76 mL H_2 /mg glucose on average, across all catalysts studied.

The activity of the catalysts was improved when ultrasonic-assisted impregnation method was used during the preparation stage. As can be seen in Table 3.2 there were no significant differences ($P > 0.05$) among the catalysts in terms of the total gas mixture, hydrogen and CO gases produced. However, there is statistically significant difference ($P < 0.05$) in CO_2 gas when PtI_2 based catalyst was used. Overall, average hydrogen

production yield was 5.30 mL H₂/mg glucose. The catalyst prepared with PtI₂ precursor produced hydrogen in relatively lower composition (74%) compared to others (83-90%).

Table 3.1. APR results of the catalysts prepared with different Pt precursors (non-sonicated)*

Pt Precursor	Total gas mixture produced (mL)	Gas Composition (mL)		
		H ₂	CO	CO ₂
H ₂ PtCl ₆	252 ±24.3 a	226 ±26.7 ab	14.8 ±2.8 a	11.7 ±2.1 a
PtBr ₂	296 ±23.4 ab	269 ±23.1 bc	13.5 ±3.1 a	13.6 ±4.6 a
PtCl ₂	349 ±25.7 b	316 ±19.7 c	19.0 ±6.1 a	14.3 ±1.9 a
PtI ₂	272 ±16.9 a	187 ±8.3 a	41.7 ±5.9 b	42.9 ±8.1 b

* Mean ± standard deviation from three replications. Values followed by same letters within a row are not significantly different (P >0.05). Variables followed by different letters are significantly different at the 5% significance level.

The presence of different halogens (Cl, Br and I) in the precursors might affect the morphology and oxygen coverage of the Pt nanoparticles (Borges, et al., 2019).

However, these parameters did not affect the surface electronic properties therefore, the catalytic activity of the catalysts was similar despite the structural differences.

Table 3.2. APR results of the catalysts prepared with different Pt precursors by ultrasound-assisted impregnation technique*.

Pt Precursor	Total gas mixture produced (mL)	Gas Composition (mL)		
		H ₂	CO	CO ₂
H ₂ PtCl ₆	379 ±23.0 a	313 ±20.8 a	23.7 ±2.9 a	18.8 ±1.3 a
PtBr ₂	300 ±53.2 a	254 ±64.5 a	28.7 ±20.8 a	16.9 ±8.0 a
PtCl ₂	330 ±28.1 a	297 ±18.7 a	17.3 ±4.7 a	15.5 ±5.6 a
PtI ₂	330 ±9.0 a	246 ±13.1 a	37.3 ±3.1 a	46.1 ±2.1 b

* Mean ± standard deviation from three replications. Values followed by same letters within a row are not significantly different (P > 0.05).

Application of ultrasonication enhanced the adsorption capacity of the precursor on graphene and led to better dispersion compared to the catalysts prepared by impregnation only. This results in finer metallic particles on the graphene as discussed in Chapter 2. The reduction in the Pt particle size leads to a lower coordination number of coordinated atoms, which affects the electronic properties and the binding energies between Pt and reaction intermediates reflecting highly active Pt sites (Frenkel, Hills, & Nuzzo, 2001; Kleis, et al., 2011). More Pt precursor molecules can enter into the deeper pores of graphene support under sonication, but some of these Pt particles may not be accessible and therefore may not effectively react with glucose to produce hydrogen.

It is clear that the use of sonication can significantly affect the performance of the catalysts and reduce catalytic differences among the catalysts prepared with different Pt precursors.

3.3.2 Effect of different metals and their bimetallic combinations with Pt

A more practical approach to reduce the cost of the catalyst is to replace some of Pt particles with non-expensive metals that do not cause considerable loss of catalytic performance. A good liquid-phase reforming catalyst for H_2 production should lead to cleavage of C-C, C-H and O-H bonds in the organic substrate (e.g. glucose) that adsorb on the catalyst surface. This catalyst should effectively remove adsorbed CO species on catalyst surface by the water-gas shift reaction ($CO + H_2O \leftrightarrow H_2 + CO_2$) and increase H_2 production to the same extent while facilitating C-C bond cleavage. However, C-O bond cleavage and hydrogenation of CO or CO_2 must be avoided (Cortright, Davda, & Dumesic, 2002). It was reported that the activity of Pt catalysts could be improved by addition of Ni, Co or Fe to a Pt/ Al_2O_3 catalyst (Huber, Shabaker, Evans, & Dumesic, 2006). In the present study, Ni and W metal particles deposited on graphene support along with and without Pt particles and catalytic activity of the resulted catalysts were evaluated by APR process. As can be seen in Table 3.3, Ni and W monometallic catalysts led to formation of less hydrogen than Pt monometallic catalyst. This is expected because Pt is known to be the best monometallic catalyst for hydrogen gas production activity and selectivity (Shabaker, Huber, Davda, Cortright, & Dumesic, 2003; Huber, Shabaker, Evans, & Dumesic, 2006).

Catalytic performance of Ni was better than W. However, when these metals were used in combination with Pt, the catalytic performance considerably increased. Although the amount of Pt was lowered to half, adding Ni or W caused positive synergy in hydrogen production activity thus, catalytic performance of bimetallic catalysts increased. It is interesting to point out that activity of Pt-W was observed to be slightly

higher than Pt-Ni (Table 3.3). It was reported in the literature that tungsten species such as W, WO₃, H₂WO₄ are active for C-C bond cleavage of cellulose (Wang & Zhang, 2013) and it was expected to exhibit higher performance in glucose, a monomer unit of cellulose and a small molecule. The comparison of the catalysts can also be clearly seen in Figure 3.1 in terms of hydrogen percentage of the gas mixture produced as well as hydrogen yield which was calculated based on the amount of glucose feed used in APR process.

Table 3.3. APR results of the catalysts prepared with different metals and combination of these metals with Pt*

Pt Precursor	Total gas mixture produced (mL)	Gas Composition (mL)		
		H ₂	CO	CO ₂
Pt	379 ±23.0 a	313 ±20.8 a	23.7 ±2.9 d	18.8 ±1.3 d
Ni	341 ±22.2 a	186 ±13.7 b	71.3 ±4.2 b	82.3 ±5.7 b
W	363 ±20.6 a	165 ±7.0 b	93.3 ±8.0 a	105 ±6.0 a
Pt-Ni	350 ±22.7 a	232 ±12.0 c	52.3 ±10.3 c	63.5 ±6.2 c
Pt-W	391 ±27.9 a	260 ±17.0 c	59.7 ±5.5 bc	69.3 ±3.5 bc

* H₂PtCl₆.6H₂O was used as Pt precursor. Catalysts were prepared by applying sonication during wet impregnation process. Mean ± standard deviation from three replications. Values followed by same letters within a row are not significantly different (P >0.05).

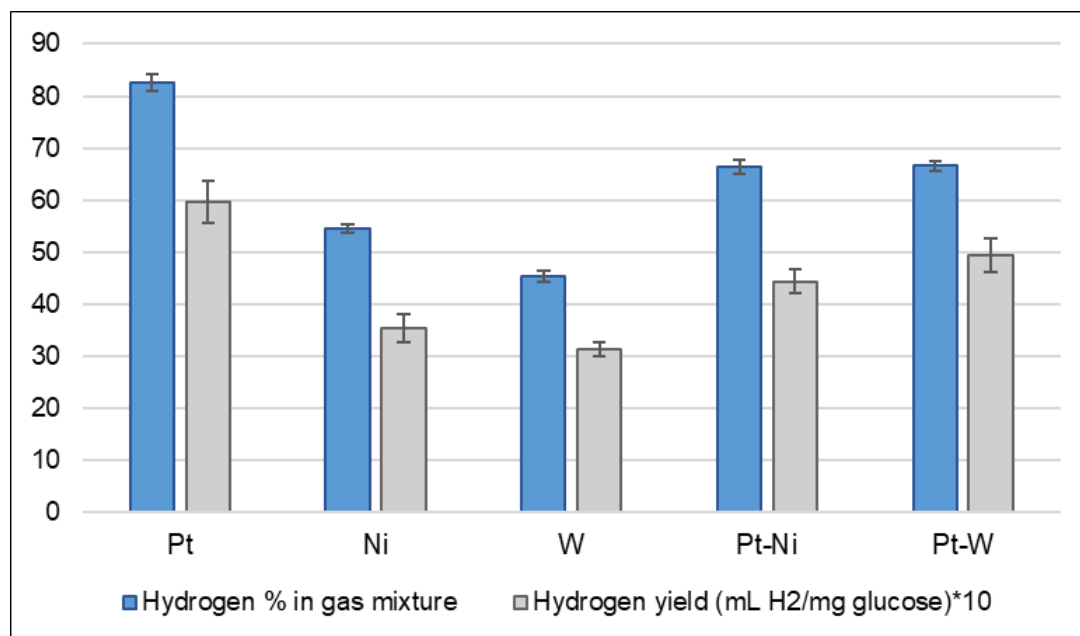


Figure 3.1. Hydrogen percentages of the gas mixtures produced and hydrogen yield obtained in mono and bimetallic catalysts.

3.4 Conclusion

The use of different Pt precursor did not change catalytic activity of Pt/graphene catalysts in terms of total gas mixture and hydrogen produced if ultrasonication was used in wet impregnation process. Although catalytic activity of monometallic Ni and W catalysts cannot comparable with monometallic Pt catalyst, combination of Ni and W metals with Pt showed positive synergy and the catalytic performance of bimetallic catalysts significantly enhanced. Hydrogen was produced in higher yield and in richer composition in Pt-Ni and Pt-W catalysts despite of reducing Pt amount to half in these catalysts.

References

- Borges, L., Lopez-Castillo, A., Meira, D., Gallo, J., Zanchet, D., & Bueno, J. (2019). Effect of the Pt precursor and loading on the structural parameters and catalytic properties of Pt. *ChemCatChem*, 11(13), 3064-3074.
- Cortright, R., Davda, R., & Dumesic, J. (2002). Hydrogen from catalytic reforming of biomass-derived hydrocarbons in liquid water. *Nature*, 418(6901), 964-967.
- Davda, R., & Dumesic, J. (2004). Renewable hydrogen by aqueous-phase reforming of glucose. *Chemical Communications*, 4(1), 36-37.
- Davda, R., Shabaker, J., Huber, G., Cortright, R., & Dumesic, J. (2003). Aqueous-phase reforming of ethylene glycol on silica-supported metal catalysts. *Applied Catalysis B: Environmental*, 43(1), 13-26.
- Frenkel, A., Hills, C., & Nuzzo, R. (2001). A view from the inside: Complexity in the atomic scale ordering of supported metal nanoparticles. *Journal of Physical Chemistry B*, 105(51), 12689-12703.
- Geng, L., Gong, J., Qiao, G., Ye, S., Zheng, J., Zhang, N., & Chen, B. (2019). Effect of metal precursors on the performance of Pt/SAPO-11 catalysts for n-dodecane hydroisomerization. *ACS Omega*, 4(7), 12598-12605.
- Huber, G., Shabaker, J., Evans, S., & Dumesic, J. (2006). Aqueous-phase reforming of ethylene glycol over supported Pt and Pd bimetallic catalysts. *Applied Catalysis B: Environmental*, 62(3-4), 226-235.
- Kaya, B., Irmak, S., Hesenov, A., Erbatur, O., & Erkey, C. (2012). Effect of support materials on supported platinum catalyst prepared using a supercritical fluid deposition technique and their catalytic performance for hydrogen-rich gas production from lignocellulosic biomass. *Bioresource Technology*.
- Kleis, J., Greeley, J., Romero, N., Morozov, V., Falsig, H., Larsen, A., . . . Jacobsen, K. (2011). Finite size effects in chemical bonding: From small clusters to solids. *Catalysis Letters*, 141(8), 1067-1071.

- Meryemoğlu, B., Hasanoğlu, A., Kaya, B., Irmak, S., & Erbatur, O. (2014). Hydrogen production from aqueous-phase reforming of sorghum biomass: An application of the response surface methodology. *Renewable Energy*.
- Meryemoglu, B., Hesenov, A., Irmak, S., Atanur, O., & Erbatur, O. (2010). Aqueous-phase reforming of biomass using various types of supported precious metal and raney-nickel catalysts for hydrogen production. *International Journal of Hydrogen Energy*.
- Nguyen, H., Lu, H., Kobayashi, E., Ishikawa, T., & Komiyama, M. (2014). Raney-nickel catalyst deactivation in supercritical water gasification of ethanol fermentation stillage and its mitigation. *Topics in Catalysis*. 57, pp. 1078-1084. Kluwer Academic Publishers.
- Ren, N., Yang, Y., Shen, J., Zhang, Y., Xu, H., Gao, Z., & Tang, Y. (2007). Novel, efficient hollow zeolitically microcapsulized noble metal catalysts. *Journal of Catalysis*, 251(1), 182-188.
- Shabaker, J., Huber, G., Davda, R., Cortright, R., & Dumesic, J. (2003). Aqueous-phase reforming of ethylene glycol over supported platinum catalysts. *Catalysis Letters*, 88(1-2), 1-8.
- Wang, A., & Zhang, T. (2013). One-pot conversion of cellulose to ethylene glycol with multifunctional tungsten-based catalysts. *Accounts of Chemical Research*, 46(7), 1377-1386.

CHAPTER 4: CONCLUSIONS AND SUGGESTIONS FOR FUTURE RESEARCH

1. The size of metal particles and their distribution on the support were considerably improved by application of sonication in catalyst preparation stage. However, different impregnation conditions (change of pH, use of organic solvent, etc.) could improve the catalysts properties further.
2. Deposition of 8 wt% metal particles on graphene was easily achieved by wet impregnation method. However, different deposition techniques/methods (e.g. deposition in supercritical carbon dioxide using organometallic metal precursors) could result in highly active catalysts.
3. Pt-Ni and Pt-W bimetallic catalysts showed increased activities and as compared to their monometallic counterparts. Different metal combinations such as Pt-Co, Pt-Sn, Pt-Mn and Pt-Fe should also be tested. Moreover, the analysis of trimetallic metal catalysts may exhibit a higher activity than the bimetallic ones, and hence reduce the cost for Pt-based catalysts.
4. Small size metal nanoparticles are easily deactivated under severe hydrothermal gasification (aqueous-phase reforming, sub- and supercritical water) conditions. This is a major drawback for high yielding hydrogen gas production. The main reasons for activity loss of supported precious metal catalysts are aggregation or poisoning of metal particles in reaction medium or coke deposition on active surfaces of the catalysts (Ren, et al., 2007). Leaching of the metal particles from support also causes loss in catalyst activity. The development of highly active catalysts with longer lifetime for hydrothermal conversion of biomass compounds to hydrogen is needed. Efforts have been made in this study focused on improving

the catalytic activity of the catalysts towards hydrogen, however, the lifetime of these catalysts should be determined in continuous APR system. In continuous APR system, catalyst is loaded and packed in a fixed-bed reactor and feed solution with a desired concentration is introduced into the reactor continuously that means the process can run uninterrupted. The quantity of feed converted to products declines as time progresses which indicates loss of catalyst activity. This stage determines lifetime of the catalyst. At that point, the reactor should be charged with new catalysts or spent catalyst should be regenerated *in-situ* or off-site.

5. Reactivity of the graphene support can be increased by different approaches.

Chemical doping is an important approach to tailor the property of graphene that can change its surface reactivity and increase its performance as catalyst support. Introduction of heteroatoms, such as nitrogen, boron, phosphorus, or sulfur atoms, into the carbon lattice of graphene by chemical doping can change the electronic properties of graphene. The nitrogen atom doping has been recognized as the most promising one because of following reasons: nitrogen atoms can create defects in graphene structure and high positive charge distribution in the nearby C atoms due to its high electron withdrawing ability, atomic sizes of nitrogen and carbon atoms are similar and five available valence electrons in nitrogen can lead to formation of valence bonds with C atoms and covalent bonding between N and C network of graphene results in more stable structure (Nicholls, et al., 2013; Guo, et al., 2010; Fan, et al., 2016). N-graphene can be prepared by either direct

synthesis (e.g. chemical vapor deposition) or post treatment (heating graphene with NH_3 at high temperature ≥ 800 °C).

References

- Fan, M., Feng, Z., Zhu, C., Chen, X., Chen, C., Yang, J., & Sun, D. (2016). Recent progress in 2D or 3D N-doped graphene synthesis and the characterizations, properties, and modulations of N species. *Journal of Materials Science*, 51(23), 10323-10349. Springer New York LLC.
- Guo, B., Liu, Q., Chen, E., Zhu, H., Fang, L., & Gong, J. (2010). Controllable N-doping of graphene. *Nano Letters*, 10(12), 4975-4980.
- Nicholls, R., Murdock, A., Tsang, J., Britton, J., Pennycook, T., Koós, A., . . . Yates, J. (2013). Probing the bonding in nitrogen-doped graphene using electron energy loss spectroscopy. *ACS Nano*, 7(8), 7145-7150.
- Ren, N., Yang, Y., Shen, J., Zhang, Y., Xu, H., Gao, Z., & Tang, Y. (2007). Novel, efficient hollow zeolitically microcapsulized noble metal catalysts. *Journal of Catalysis*, 251(1), 182-188.